AD-A170 042 TURBULENCE MODELING FOR STEADY THREE-DIMENSIONAL SUPERSONIC FLOWS(U) DELAWARE UNIV NEWARK DEPT OF MECHANICAL AND AEROSPACE ENGINEERING 1/1

UNCLASSIFIED J E DANBERG ET AL. JUN 86 BRL-CR-553 F/G 20/4 NL

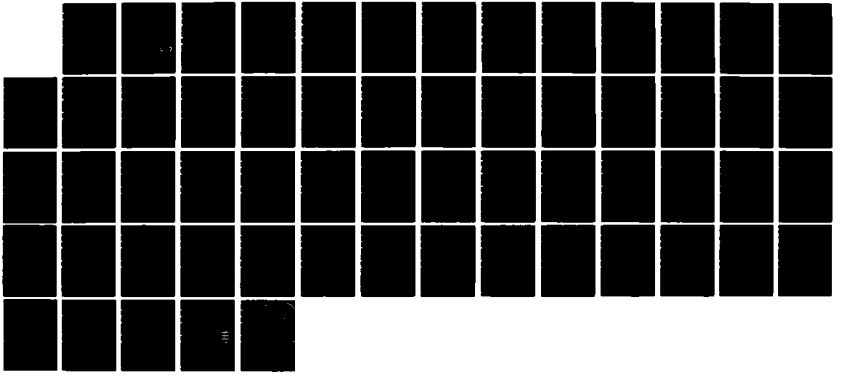

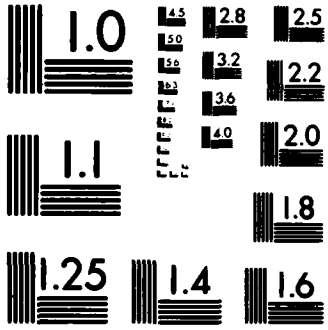

MICROCOPY RESOLUTION TEST CHART
NATIONAL BUREAU OF STANDARDS-1963-A

US ARMY
MATERIEL
COMMAND

CONTRACT REPORT BRL-CR-553

TURBULENCE MODELING FOR STEADY THREE-DIMENSIONAL SUPERSONIC FLOWS

University of Delaware
Deparment of Mechanical & Aerospace Engineering
Newark, Delaware 19716

June 1986

US ARMY BALLISTIC RESEARCH LABORATORY
ABERDEEN PROVING GROUND, MARYLAND

Destroy this report when it is no longer needed.
Do not return it to the originator.

Additional copies of this report may be obtained from the National Technical Information Service, U. S. Department of Commerce, Springfield, Virginia 22161.

The findings in this report are not to be construed as an official Department of the Army position, unless so designated by other authorized documents.

The use of trade names or manufacturers' names in this report does not constitute indorsement of any commercial product.

UNCLASSIFIED

SECURITY CLASSIFICATION OF THIS PAGE (When Data Entered)

REPORT DOCUMENTATION PAGE	READ INSTRUCTIONS BEFORE COMPLETING FORM
1. REPORT NUMBER Contract Report BRL-CR-553	2. GOVT ACCESSION NO. AD-A170042
	3. RECIPIENT'S CATALOG NUMBER
4. TITLE (and Subtitle) TURBULENCE MODELING FOR STEADY THREE-DIMENSIONAL SUPERSONIC FLOWS	5. TYPE OF REPORT & PERIOD COVERED Final
	6. PERFORMING ORG. REPORT NUMBER
7. AUTHOR(s) James E. Danberg,* Paul van Gulick, Jin Kim	8. CONTRACT OR GRANT NUMBER(s) DAAK-79-C-0018
9. PERFORMING ORGANIZATION NAME AND ADDRESS University of Delaware Department of Mechanical & Aerospace Engineering Newark, Delaware 19716	10. PROGRAM ELEMENT, PROJECT, TASK AREA & WORK UNIT NUMBERS RDT&E 1L161102AH43
11. CONTROLLING OFFICE NAME AND ADDRESS U.S. Army Ballistic Research Laboratory ATTN: SLCBR-DD-T Aberdeen Proving Ground, Maryland 21005-5066	12. REPORT DATE June 1986 13. NUMBER OF PAGES 59
14. MONITORING AGENCY NAME & ADDRESS(if different from Controlling Office)	15. SECURITY CLASS. (of this report) UNCLASSIFIED 15a. DECLASSIFICATION DOWNGRADING SCHEDULE

16. DISTRIBUTION STATEMENT (of this Report)

Approved for public release, distribution unlimited.

17. DISTRIBUTION STATEMENT (of the abstract entered in Block 20, if different from Report)

18. SUPPLEMENTARY NOTES

* Employed by the Ballistic Research Laboratory
Aberdeen Proving Ground, MD
21005-5066

19. KEY WORDS (Continue on reverse side if necessary and identify by block number)

Turbulence Modeling
Numerical Modeling
Parabolized Navier Stokes
Supersonic Flow
3D Flow

20. ABSTRACT (Continue on reverse side if necessary and identify by block number)

The Jones and Launder two-equation model of turbulence has been formulated and applied to the solution of supersonic, three-dimensional flow and the results compared to experimental data. Two solution techniques were studied, the boundary layer theory approach and the parabolized Navier-Stokes Method formulated in a body fitted coordinate system.

The K-E turbulence model results ~~have been~~ compared with an algebraic

DD FORM 1 JAN 73 1473 EDITION OF 1 NOV 65 IS OBSOLETE

UNCLASSIFIED

SECURITY CLASSIFICATION OF THIS PAGE (When Data Entered)

20. ABSTRACT (Continued)

turbulence model as applied to the prediction of flow about a spinning ogive-cylinder-boattail configuration. The K-E model gave slightly superior results in both the boundary layer and PNS computations.

Rotta's non-isotropic theory for the Reynolds stresses was incorporated into the formulation. Results for the small angle of attack configuration showed little effect of non-isotropy. The cross flow properties are the most strongly affected.

Bradshaw's streamline curvature theory was also considered and the results show negligible influence for the present case.

TABLE OF CONTENTS

LIST OF ILLUSTRATIONS

I. INTRODUCTION

The primary motivation for this work is to explore turbulence models for high speed, three-dimensional flows such as those which occur in the vicinity of artillery projectiles. The basic geometry is axisymmetric but at angle of attack or yaw. At high spin rates, the three-dimensional effects are significant. The range of angles of attack is usually small for a stable projectile but practical geometries often involve surface irregularities such as fuses and rotating bands. These surface perturbations sometimes lead to local regions of separation so that it is desirable that the model of turbulence be extendable to such conditions. Finally the projectile base flow has a very significant effect on the projectile drag and therefore a generally useful model should be applicable in the wake region.

The turbulence model must be applicable to compressible flow because most artillery launching speeds are supersonic. The lower end of the speed range, however, must also encompass transonic Mach numbers because this is often a critical flight condition which must be studied in detail.

Numerical techniques for investigating projectile flow fields have been developing rapidly over the past 15 years; starting with Euler inviscid flow solutions coupled with boundary layer techniques and currently concentrating on various forms of the thin shear layer Navier-Stokes codes which solve the inviscid and viscous field at the same time. The methods of primary interest for the turbulence modeling considered here are: the three-dimensional boundary layer technique developed by Dwyer and Sanders,[1] the parabolized Navier-Stokes technique of Schiff and Steger[2] with the numerical algorithm based on the work of Beam and Warming[3] as well as the unsteady transonic Navier-Stokes technique of Pulliam, Steger and Nietubicz.[4] [5]

---

1. *Dwyer, H.A., and Sanders, B.R., "Magnus Forces on Spinning Supersonic Cones. Part 1: the Boundary Layer," BRL Contractor Report, ARBRL-CR-248, July 1975.*

2. *Schiff, L.B., and Steger, J.L., "Numerical Simulation of Steady Supersonic Viscous Flow," AIAA Paper 79-0130, January 1979.*

3. *Beam, R.M., and Warming, R.F., "An Implicit Factored Scheme for Hyperbolic Systems in Conservation-Law Form," J. of Computational Physics, Vol. 22, 1976.*

4. *Pulliam, T.H., and Steger, J.L., "On Implicit Finite-Difference Simulations of Three-Dimensional Flow," AIAA Journal, Vol. 18, 2, pp. 159-167, February 1980.*

5. *Nietubicz, C.J., Pulliam, T.H., and Steger, J.L., "Numerical Solution of the Azimuthal-Invariant Thin-Layer Navier-Stokes Equations," AIAA Paper 79-0010, January 1979.*

Initially these numerical methods have employed algebraic turbulence models based on the mixing length theory of Prandtl.[6] These have been modified for compressibility and extended to include effects of heat transfer, pressure gradient and many other effects. One of the main criticisms of these methods is that they are local models which do not account for the convection and diffusion of turbulence. In order to include more of the physics of turbulence in the mathematical models, the 1- and 2-differential equation techniques were developed. A number of surveys[7] [8] [9] of the development and status of all these methods are available and therefore no discussion is required here. The K-E model of Jones and Launder[10] was selected as the non-local model to be tested in the above numerical codes as a representative differential equation technique.

This report consists of three main sections: the first contains a review of the three-dimensional, turbulent equations of motion aimed at clarifying the assumptions inherent in their subsequent use, the application to the three-dimensional boundary layer equations and finally their application to the steady, parabolized Navier-Stokes equations. The inclusion of the K-E equation to the boundary layer is based on the work of van Gulick[11] [12] and the application to the PNS equations has been reported by Kim.[13] Concurrently,

---

6. *Schlichting, H., "Boundary Layer Theory," 7th Edition, McGraw-Hill Book Co., 1979.*

7. *Launder, B.E., and Spalding, D.B., "Mathematical Models of Turbulence," Academic Press, Inc., 1972.*

8. *Rubesin, M.W., "Numerical Turbulence Modeling," AGARD Lecture Series No. 86 on Computational Fluid Dynamics, pp. 3-1 to 3-37, April 1977.*

9. *Reynolds, W.C., "Computation of Turbulent Flows," Ann. Rev. Fluid Mech., Vol. 8, pp. 183-208, 1976.*

10. *Jones, W.P., and Launder, B.E., "The Caluculation of Low Reynolds Number Phenomena with a Two Equation Model of Turbulence," Int. J. Heat and Mass Transfer, Vol. 16, 1973.*

11. *Van Gulick, P., "Application of the K-E Turbulence Model to a Boundary Layer Solution for Flow About a Spinning Yawed Projectile at Mach 3," Masters Thesis, Mechanical and Aerospace Engineering Department, University of Delaware, June 1983.*

12. *Van Gulick, P., and Danberg, J.E., "Application of the K-E Turbulence Model to a Boundary Layer Solution for Flow About a Spinning Yawed Projectile at Mach 3," Proceedings 12th Southeastern Conference on Theoretical and Applied Mechanics, May 1984.*

13. *Kim, J., "Computation of Three-Dimensional Turbulent Flow with Parabolized Navier-Stokes Equations and K-E Turbulence Model," Masters Thesis, Mechanical and Aerospace Engineering Department, University of Delaware, January 1984.*

the K-E technique has been tested in the unsteady, transonic Navier-Stokes problem by Sahu[14] but discussion of his work is not considered here.

II. TURBULENT COMPRESSIBLE EQUATIONS OF MOTION

A. Mean Flow Equations

The starting point in the derivation of the turbulent flow equations of motion are the compressible, laminar Navier-Stokes equations (including continuity, energy and equation of state).

Continuity

$$\frac{\partial \rho}{\partial t} + \frac{\partial}{\partial x_j} (\rho u_j) = 0 \tag{1}$$

Momentum

$$\frac{\partial (\rho u_i)}{\partial t} + \frac{\partial}{\partial x_j} (\rho u_i u_j) = - \frac{\partial p}{\partial x_j} + \frac{\partial \tau_{ij}}{\partial x_j} \tag{2}$$

Energy

$$\frac{\partial (\rho H)}{\partial t} + \frac{\partial}{\partial x_j} (\rho H u_j) = \frac{\partial p}{\partial t} + \frac{\partial}{\partial x_j} (u_i \tau_{ij} - q_j) \tag{3}$$

Constitutive equations

$$\tau_{ij} = \mu \left[\frac{\partial u_i}{\partial x_j} + \frac{\partial u_j}{\partial x_i} - \frac{2}{3} \frac{\partial u_k}{\partial x_k} \delta_{ij} \right] \tag{4}$$

$$q_j = - k \frac{\partial T}{\partial x_j} \tag{5}$$

Definition of total enthalpy

$$H = e_{int} + p/\rho + \frac{1}{2} u_i u_i \tag{6}$$

---

14. *Sahu, J., "Navier-Stokes Computational Study of Axisymmetric Transonic Turbulent Flows with a Two-Equation Model of Turbulence," Ph. D. Dissertation, Mechanical and Aerospace Engineering Department, University of Delaware, June 1984.*

Equations of state

$$p = \rho RT \tag{7}$$

$$h = C_p T. \tag{8}$$

Since these equations cannot be solved at this time for fully turbulent flow because the length and time scales of the motion are too disparate, solutions are sought to altered equations produced by averaging over time and neglecting or modeling various terms. The derivation used here is based on mass-weighted time-averaging.[15] [16] By definition the mass-weighted mean (denoted by tilde) is

$$\tilde{a} = \overline{\rho a} / \bar{\rho} \tag{9}$$

where an over bar is a conventional time average. We will use a single prime to indicate the fluctuating part in the mass-weighted variable, i.e.:

$$a(\vec{r},t) = \tilde{a}(\vec{r}) + a'(\vec{r},t) \tag{10}$$

and a double prime is used to denote the fluctuating part in a simple time average:

$$a(\vec{r},t) = \bar{a}(\vec{r}) + a''(\vec{r},t) \tag{11}$$

It follows then that

$$\overline{\rho a'} = 0 \text{ and } \overline{a''} \equiv 0$$

but $\overline{a'} \neq 0$. Based on these definitions one can derive the following equations:

---

15. *Cebeci, T., and Smith, A.M.O., "Analysis of Turbulent Boundary Layers," Academic Press, Inc., 1974.*

16. *Rubesin, M.W., "A One-Equation Model of Turbulence for Use with the Compressible Navier-Stokes Equations," NASA TMX-73, 1976.*

Continuity

$$\frac{\partial \bar{\rho}}{\partial t} + \frac{\partial}{\partial x_j} (\bar{\rho}\, \tilde{u}_j) = 0 \tag{12}$$

Momentum

$$\frac{\partial \bar{\rho}\tilde{u}_j}{\partial t} + \frac{\partial}{\partial x_j} (\bar{\rho}\tilde{u}_i\tilde{u}_j) = - \frac{\partial \bar{p}}{\partial x_j} + \frac{\partial}{\partial x_j} (\bar{\tau}_{ij} - \overline{\rho u_i' u_j'}) \tag{13}$$

where $-\overline{\rho u_i' u_j'}$ is the Reynolds stress tensor. These additional unkowns render the set of equations insufficient and therefore a generalization of the Boussinesq formula is introduced. If we write

$$- \overline{\rho u_i' u_j'} = \mu_t \left[\frac{\partial \tilde{u}_i}{\partial x_j} + \frac{\partial \tilde{u}_j}{\partial x_i} \right] + A\, \delta_{ij}$$

where A is an invariant of the Reynolds stress tensor. The trace of the tensor gives,

$$A = - \frac{2}{3} \frac{\partial \tilde{u}_k}{\partial x_k} - \frac{1}{3} \overline{\rho u_i' u_i'} \, .$$

Thus, since

$$\tilde{d}_{ij} = \frac{\partial \tilde{u}_i}{\partial x_j} + \frac{\partial \tilde{u}_j}{\partial x_i} - \frac{2}{3} \frac{\partial \tilde{u}_k}{\partial x_k}\, \delta_{ij} \, ,$$

we can write the Reynolds stress as

$$- \overline{\rho u_i' u_i'} = \mu_t\, \tilde{d}_{ij} - \frac{2}{3}\, \bar{\rho}\, \tilde{K}\, \delta_{ij} \tag{14}$$

where $\tilde{K}$ is the mass weighted average kinetic energy.

$$\tilde{K} = 0.5\, \overline{\rho u_i' u_i'} \, / \, \bar{\rho} \, .$$

The molecular stress $\tilde{\tau}_{ij}$ can also be written in terms of d_{ij} as follows.

$$\bar{\tau}_{ij} = \bar{\mu}\, \tilde{d}_{ij} + \overline{\mu d_{ij}'} \, . \tag{15}$$

The second term on RHS of this equation is the interaction of the variable transport property and the fluctuating velocities and is usually neglected.

If this term can be ignored then the resulting equation for the combined molecular and turbulent stress becomes

$$\bar{\tau}_{ij} - \overline{\rho u_i' u_j'} = (\bar{\mu} + \mu_t)\, \tilde{d}_{ij} - \frac{2}{3}\, \bar{\rho}\, \tilde{K}\, \delta_{ij} \quad . \tag{16}$$

In most algebraic turbulence models which do not compute fluctuating quantities, it is not possible to account for the last term involving the turbulent kinetic energy. Neglecting this term has the advantage that the total shear stress is proportional to the mass weighted average of d_{ij} and the equations derived for compressible laminar flow may be used to compute turbulent flow by simply replacing the viscosity coefficient $\bar{\mu}$ by the sum of the molecular and turbulent viscosity $\bar{\mu} + \mu_t$. This assumption has been made in the computations reported here but the problem is pointed out and needs further investigation.

The turbulent "eddy" viscosity, μ_t, can be dimensionally described in terms of a density times a characteristic velocity times a characteristic length. In the algebraic turbulence models, the characteristic velocity is generally proportional to the mean velocity gradient so that

$$\mu_t = \bar{\rho}\, \ell^2\, \frac{\partial \tilde{u}}{\partial y} \, . \tag{17}$$

In the "two equation" turbulence models considered here, the velocity scale is related to the square root of the kinetic energy of turbulence, $\tilde{K}^{1/2}$. The length scale is equal to $\tilde{K}^{3/2}/\tilde{E}$, where $\tilde{E}$ is the dissipation rate, so that

$$\mu_t = c_\mu\, \bar{\rho}\, \tilde{K}^2/\tilde{E} \tag{18}$$

where c_μ is assigned the value $c_\mu = 0.09$. A comprehensive discussion of algebraic, one- and two-equation models of turbulence is contained in the survey by Launder and Spalding.[7]

The energy equation is modified recognizing that

$$\rho H = e + p \tag{19}$$

where

$$e = \rho e_{int} + 1/2\, \rho u_i u_i \tag{20}$$

or the total energy per unit volume of the flow (e_{int} = internal energy/mass = $c_v T$). Consistent with the averaging process used previously, the turbulent flow energy equation becomes

$$\frac{\partial}{\partial t}(\bar{e} + \bar{p}) + \frac{\partial}{\partial x_j}[(\bar{e} + \bar{p})\tilde{u}_j] =$$

$$\frac{\partial \bar{p}}{\partial t} + \frac{\partial}{\partial x_j}(-\bar{q}_j - \overline{(e + p)u_j''} + \tilde{u}_i \bar{\mu}\, \tilde{d}_{ij} \tag{21}$$

$$+ \tilde{u}_i\, \overline{\mu d_{ij}''} + \overline{u_i'' \tau_{ij}}\,).$$

Fourier's law becomes

$$\bar{q}_j = -(\bar{k} + k'')\frac{\partial}{\partial x_j}(\bar{T} + T''). \tag{22}$$

The mean molecular heat flux and stress work are taken to be

$$\bar{k}\frac{\partial \bar{T}}{\partial x_j} + \tilde{u}_i \bar{\mu}\, \tilde{d}_{ij}\,. \tag{23}$$

In analogy with the Boussinesq representation for the Reynolds stresses we write the following for the heat flux and shear work:

$$(\bar{k} + k_t)\frac{\partial \bar{T}}{\partial x_j} + \tilde{\mu}_i\, \tilde{\tau}_{ij} = -\bar{q}_j - \overline{(e + p)u_j''} + \tilde{u}_i \tilde{\tau}_{ij} + \overline{u_i'' \tau_{ij}} \tag{24}$$

so the the turbulent heat flux is determined by

$$k_t \frac{\partial \bar{T}}{\partial x_j} = \overline{k'' \frac{\partial T''}{\partial x_j}} - \overline{(e + p)u_j''} + \overline{u_i'' \tau_{ij}} + \overline{u_i \mu d_{ij}''}\,, \tag{25}$$

It is convenient to eliminate temperature from the final equation using

$$T = a^2/\gamma R = \frac{a^2}{(\gamma - 1)C_p} \tag{26}$$

which is averaged to give:

$$\bar{T} = \overline{a^2}/[(\gamma - 1)C_p]. \tag{27}$$

The thermal conductivities are also eliminated by introducing the molecular and turbulent Prandtl numbers

$$Pr = C_p \bar{\mu}/\bar{k} \ , \tag{28}$$

and

$$Pr_t = C_p \mu_t / k_t . \tag{29}$$

Thus the final form of the energy equation for turbulent flow becomes:

$$\frac{\partial \bar{e}}{\partial t} + \frac{\partial}{\partial x_j}\left[\tilde{u}_j(\bar{e}+\bar{p})\right] = \frac{\partial}{\partial x_j}\left[\frac{1}{(\gamma-1)}\left[\frac{\bar{\mu}}{P_r} + \frac{\mu_t}{P_{r_t}}\right]\frac{\partial \overline{a^2}}{\partial x_j}\right]. \tag{30}$$

The reason for developing the mean flow Navier-Stokes equations in the above form is to define and emphasize clearly some of the underlying assumptions which have been made in using the equations in this form.

1. The velocity components, $\tilde{u}_j$, are mass-weighted time averages. Since most solutions do not provide information regarding the density fluctuations it is not possible to relate $\bar{u}_j$ to $\tilde{u}_j$, the physical velocity.

2. A term involving the kinetic energy of turbulence has been neglected in formulating the Boussinesq approximation to the Reynolds stresses, i.e.:

$$-\frac{2}{3}\bar{\rho}\tilde{K}\delta_{ij}.$$

Although this term applies to the normal stresses and therefore may be expected to be relatively unimportant, it should be possible in the K-E models to test its significance.

3. $\mu_t \tilde{d}_{ij} = \overline{\mu d'_{ij}} - \overline{\rho u'_i u'_j}$

As already pointed out in the mass-weighted average derivation, $\overline{d'_{ij}} \neq 0$ and thus even if $\mu = \bar{\mu}$, the $\overline{\mu d'_{ij}}$ term is not obviously zero and $\mu_t \tilde{d}_{ij}$ represents more than the conventional form of the Reynolds stresses

4. The turbulent heat flux, equation (25), also contains a number of additional terms which would not appear in incompressible flow even if k'' is negligible.

5. The definition of the mean total energy can be used to provide an equation for the mean pressure

$$\bar{p} = (\gamma-1)\left[\bar{e} - \frac{1}{2}\bar{\rho}\tilde{u}_i\tilde{u}_i - \frac{1}{2}\overline{\rho u_i' u_i'}\right].$$

In most computational work, the kinetic energy of turbulence in this equation is ignored in the evaluation of the mean pressure. This is necessary when using the algebraic turbulence models but could be accounted for when using the K-E equations.

6. In general, the fluctuations in transport properties k'' and M'' are neglected (see for example References 17 and 18). However, the only justification is mathematical convenience.

B. Turbulent Kinetic Energy Equation

Multiplying the momentum equation by the instantaneous velocity, taking the time average, considering only the terms where j = i and subtracting the mean kinetic energy, one obtains an equation for the kinetic energy of the turbulent fluctuations

$$\frac{D}{Dt}\left[\frac{\overline{\rho u_i' u_i'}}{2}\right] = \frac{\partial}{\partial x_k}\left[\overline{u_k'\left[\frac{\rho u_i' u_i'}{2}\right]}\right] - \overline{u_i'\frac{\partial p}{\partial x_i}} + \overline{u_i'\frac{\partial \tau_{ik}}{\partial x_k}} - \overline{\rho u_i' u_k'}\frac{\partial \tilde{u}_i}{\partial x_k} \quad (31)$$

which can be rewritten as

$$\frac{D}{Dt}\left[\frac{\overline{\rho u_i' u_i'}}{2}\right] = -\frac{\partial}{\partial x_j}\left[\overline{u_j'\left(\frac{1}{2}\rho u_i' u_i'\right)} + \overline{u_j' p} - \overline{u_i'\tau_{ij}}\right]$$

$$+ \overline{p\frac{\partial u_i'}{\partial x_i}} - \overline{\tau_{ij}\frac{\partial u_i'}{\partial x_j}} - \overline{\rho u_i' u_k'}\frac{\partial \tilde{u}_i}{\partial x_k}. \quad (32)$$

The four terms on the right hand side represent the diffusion of turbulent kinetic energy, tendency toward isotropy, dissipation and production terms

---

17. *White, F.M., "Viscous Fluid Flow," McGraw-Hill Book Company, 1974.*

18. *Schubauer, G.B., and Tchen, C.M., "Turbulent Flow," Turbulent Flow and Heat Transfer, Ed. C. C. Lin, Princeton Series on High Speed Aerodynamics and Jet Propulsion, Princeton University Press, 1959.*

respectively. In this derivation, the dependent variable is the kinetic energy per unit volume $\rho u_i'' u_i''/2$ obtained for incompressible flow. In the limit that $\rho \rightarrow$ constant and thus $u_i'' \rightarrow u_i''$ with $\tau_{ij} = \bar{\tau}_{ij} + \tau_{ij}''$, the above equation reduces to the usual incompressible form. Thus for the compressible case it is only necessary to rewrite the kinetic energy in terms of the mass weighted average

$$\tilde{K} = 0.5 \, \overline{\rho u_i'' u_i''}/\bar{\rho} \quad . \tag{33}$$

The tendency-toward-isotropy term is ignored in forming a model equation to represent equation (32). The dissipation is also considered as a mass-weighted average so that

$$\overline{\tau_{ij} \frac{\partial u_i''}{\partial x_j}} = \bar{\rho} \, \tilde{\varepsilon} \tag{34}$$

and finally the production term is written using the Boussinesq form as

$$-\overline{\rho u_i'' u_k''} \frac{\partial \tilde{u}_i}{\partial x_k} = \mu_t \, \tilde{d}_{ik} \frac{\partial \tilde{u}_i}{\partial x_k} \tag{35}$$

(the contribution of $\overline{\mu d_{ij}''}$ has also been neglected). Thus the model kinetic energy equation becomes

$$\frac{D}{Dt} (\bar{\rho} \, \tilde{K}) = \frac{\partial}{\partial x_j} \left[\left[\bar{\mu} + \frac{\mu_t}{\sigma_k} \right] \frac{\partial \tilde{K}}{\partial x_j} \right] - \bar{\rho} \, \tilde{\varepsilon} + \mu_t \, \tilde{d}_{ik} \frac{\partial \tilde{u}_i}{\partial x_k} \tag{36}$$

where according to Jones and Launder[10], $\sigma_K = 1.0$.

C. Dissipation of Turbulent Energy Model Equation

The dissipation rate of turbulent kinetic energy ε is written in analogy to the model kinetic energy of turbulence equation as:

$$\frac{D}{Dt}(\bar{\rho} \, \tilde{\varepsilon}) = \frac{\partial}{\partial x_j} \left[\left[\bar{\mu} + \frac{\mu_t}{\sigma_\varepsilon} \right] \frac{\partial \tilde{\varepsilon}}{\partial x_j} \right] - C_2 \bar{\rho} \frac{\tilde{\varepsilon}^2}{\tilde{K}} + C_1 \frac{\tilde{\varepsilon}}{\tilde{K}} \mu_t \tilde{d}_{ik} \frac{\partial \tilde{u}_i}{\partial x_k} \, . \tag{37}$$

The production and dissipation terms have the same form as their kinetic energy equation counterparts but scaled by $\tilde{\varepsilon}/\tilde{K}$ and multiplied by constants:[10] $C_1 = 1.44$, $C_2 = 1.92$ and $\sigma_\varepsilon = 1.3$.

D. Low Reynolds Number Effects

In the form indicated by equations (36) and (37), the dissipation remains finite at the wall and is balanced by the diffusion term. It is desirable for computational purposes to redefine $\tilde{\varepsilon}$ such that its value at a bounding wall is zero. This is achieved by adding a term to the definition of $\tilde{\varepsilon}$ which is according to Jones and Launder[10]

$$\tilde{E} = \tilde{\varepsilon} - 2\nu \left[\frac{\partial}{\partial x_k} (\tilde{K}^{1/2})\right]^2 . \tag{38}$$

If $\tilde{\varepsilon}$ is replaced by $\tilde{E}$ in the dissipation rate equation, the diffusion term remains finite at the wall. The equation can be balanced by adding a term as follows

$$c_3 \bar{\nu} \mu_t \left[\frac{\partial^2 \tilde{u}_i}{\partial x_i \partial x_j}\right]^2 . \tag{39}$$

The modified K-E equations becomes

$$\frac{D}{Dt} (\bar{\rho} \tilde{K}) = \frac{\partial}{\partial x_j}\left[\left[\bar{\mu} + \frac{\mu_t}{\sigma_k}\right] \frac{\partial \tilde{K}}{\partial x_j}\right] - \bar{\rho} \tilde{E} + \mu_t \tilde{d}_{ik} \frac{\partial \tilde{u}_i}{\partial x_k} - 2\bar{\rho} \bar{\nu} \left[\frac{\partial}{\partial x_k} (K^{1/2})\right]^2$$

$$\frac{D}{Dt} (\bar{\rho} \tilde{E}) = \frac{\partial}{\partial x_j}\left[\left[\bar{\mu} + \frac{\mu_t}{\sigma_E}\right] \frac{\partial \tilde{E}}{\partial x_j}\right] - c_2 \bar{\rho} \frac{\tilde{E}^2}{\tilde{K}} + c_1 \frac{\tilde{E}}{\tilde{K}} \mu_t \tilde{d}_{ik} \frac{\partial \tilde{u}_i}{\partial x_k} \tag{40}$$

$$+ c_3 \bar{\nu} \mu_t \left[\frac{\partial^2 \tilde{u}_i}{\partial x_i \partial x_j}\right]^2 .$$

Van Gulick[11] using a series expansion technique has shown that $\tilde{K} = O(y^2)$ as $y \to 0$, and that $\tilde{E} = O(y)$ with the result that $\mu_t = O(y^3)$ as suggested by White.[17] However, van Gulick's experience with the boundary layer equations showed that the $\tilde{K}^{1/2}$ term made the numerical solution highly unstable. As a result, he adopted a proposal by Chien[19] in which $\tilde{\varepsilon}$ was changed to

---

19. *Chien, K-Y., "Predictions of Channel and Boundary Layer Flows with a Low-Reynolds-Number Turbulence Model," AIAA Journal, Vol. 20, No. 1, January 1982.*

$$\tilde{E} = \tilde{\varepsilon} - 2\bar{\nu}\,\tilde{K}/y^2 \tag{41}$$

and the added term in the $\tilde{E}$ equation becomes

$$-2\nu \frac{\tilde{E}}{y^2} \exp\left(-\frac{1}{2} y^+\right) \tag{42}$$

where $y^+ = u_\tau y/\nu_w$. This term becomes small very rapidly as y increases and has the correct form to balance the diffusion term at y = 0. Chien also suggested that c_μ in the equation for μ_t include a damping term similar to that of the van Driest damping factor

$$c_\mu = 0.09\,(1 - \exp(-0.01\, y^+))$$

which maintains $\mu_t = O(y^3)$ near y = 0.

E. Rotta's Three-Dimensional Stress Tensor Model

The Boussinesq postulation used to simplify the writing of the Reynolds stress terms in the momentum equation implies that the eddy viscosity produced by turbulence is isotropic and that the differences in the various components of the Reynolds stress are just determined by the components of the strain rate tensor, d_{ij}. In general, the full equation for the Reynolds stress is a complicated tensor relation which could permit Reynolds stresses in three dimensions which are not aligned with the local mean rate of strain.

Employing the incompressible equations, Rotta[20] asserts that the non-isotropy of the flow is due to the pressure strain term which he writes as two separate components:

$$\frac{p''}{\rho}\left[\frac{\partial u''}{\partial y} + \frac{\partial v''}{\partial x}\right] = \frac{p_m''}{\rho}\left[\frac{\partial u''}{\partial y} + \frac{\partial v''}{\partial x}\right] + \frac{p_t''}{\rho}\left[\frac{\partial u''}{\partial y} + \frac{\partial v''}{\partial x}\right],$$

$$\frac{p''}{\rho}\left[\frac{\partial w''}{\partial y} + \frac{\partial v''}{\partial z}\right] = \frac{p_m''}{\rho}\left[\frac{\partial w''}{\partial y} + \frac{\partial v''}{\partial z}\right] + \frac{p_t''}{\rho}\left[\frac{\partial w''}{\partial y} + \frac{\partial v''}{\partial z}\right]. \tag{43}$$

---

20. *Rotta, J.C., "A Family of Turbulence Models for Three-Dimensional Thin-Shear Layers," Symposium of Turbulent Shear Flows, University Park, Pennsylvania, 1977.*

The terms involving p_m'' were assumed to be proportional to the mean strain rates in streamline coordinates and to $\overline{v''^2}$. After transforming from streamline to general Cartesian coordinates he found

$$\overline{\frac{p_m''}{\rho}\left[\frac{\partial u''}{\partial y}+\frac{\partial v''}{\partial x}\right]} = \left[\chi_{xx}\frac{\partial \bar{u}}{\partial y}+\chi_{xz}\frac{\partial \bar{w}}{\partial y}\right]\overline{v''^2}$$

$$\overline{\frac{p_m''}{\rho}\left[\frac{\partial w''}{\partial y}+\frac{\partial v''}{\partial x}\right]} = \left[\chi_{zx}\frac{\partial \bar{u}}{\partial y}+\chi_{zz}\frac{\partial \bar{w}}{\partial y}\right]\overline{v''^2} \qquad (44)$$

where

$$\chi_{xx} = (\chi_{ss}\bar{u}^2 + \chi_{nn}\bar{w}^2)/(\bar{u}^2+\bar{w}^2)$$

$$\chi_{xz} = (\chi_{ss} - \chi_{nn})\,\bar{u}\,\bar{w}/(\bar{u}^2+\bar{w}^2) \qquad (45)$$

$$\chi_{zz} = (\chi_{ss}\bar{w}^2 + \chi_{nn}\bar{u}^2)/(\bar{u}^2+\bar{w}^2)$$

and where χ_{ss} and χ_{nn} are constants of proportionality in the streamline coordinate system.

The other factors in the pressure-strain terms involving p_t'' were presumed to be proportioned to the local Reynolds stress, i.e.:

$$\overline{\frac{p_t''}{\rho}\left[\frac{\partial u''}{\partial y}+\frac{\partial v''}{\partial x}\right]} = -K_p\sqrt{\tilde{K}}\;\overline{u''v''}\;/L$$

$$\overline{\frac{p_t''}{\rho}\left[\frac{\partial w''}{\partial y}+\frac{\partial v''}{\partial z}\right]} = -K_p\sqrt{K}\;\overline{w''v''}\;/L \qquad (46)$$

where K_p is a constant of proportionality. Neglecting all the other terms in the equation for the Reynolds stresses Rotta, determined the stress components as:

$$-\overline{\rho u''v''} = \frac{\mu_t}{(\bar{u}^2+\bar{w}^2)}\left[(\bar{u}^2+F\bar{w}^2)\frac{\partial \bar{u}}{\partial y}+(1-F)\,\bar{u}\,\bar{w}\frac{\partial \bar{w}}{\partial y}\right]$$

$$-\overline{\rho w''v''} = \frac{\mu_t}{(\bar{u}^2+\bar{w}^2)}\left[(1-F)\,\bar{u}\,\bar{w}\frac{\partial \bar{u}}{\partial y}+(\bar{w}^2+F\,\bar{u}^2)\frac{\partial \bar{w}}{\partial y}\right] \qquad (47)$$

where μ_t is the isotropic eddy viscosity corresponding to F = 1 and where, in general,

$$F = \frac{1 - x_{nn}}{1 - x_{ss}} \quad . \tag{48}$$

F is thus a parameter to be selected by comparison with experimental data. Rotta suggested a value of 0.5.

F. Effect of Non-Isotropy on the $\tilde{K}$-Equation Production Term

Van Gulick applied the Rotta theory to the boundary layer form of the K-E equations where the production term can be written as

$$P = \overline{\rho u'v'} \frac{\partial \tilde{u}}{\partial y} + \overline{\rho w'v'} \frac{\partial \tilde{w}}{\partial y} \quad . \tag{49}$$

If it is assumed that the above analysis holds at least approximately for the compressible case, then P can be written

$$P = \mu_t \left[\left[\frac{\partial \tilde{u}}{\partial y}\right]^2 + \left[\frac{\partial \tilde{w}}{\partial y}\right]^2 \right.$$

Isotropic part

$$\left. - (1-F) \left[\left[\frac{\partial \tilde{u}}{\partial y}\right]^2 + \left[\frac{\partial \tilde{w}}{\partial y}\right]^2 - \frac{\left[\tilde{u}\frac{\partial \tilde{u}}{\partial y} + \tilde{w}\frac{\partial \tilde{w}}{\partial y}\right]}{\left[\tilde{u}^2 + \tilde{w}^2\right]} \right] \right] \quad . \tag{50}$$

Non-Isotropic part

In the limit as $y \to 0$, $\tilde{u} \to 0$ and $\tilde{w} \to \Omega r$ (circumferential velocity due to spin):

$$P \to \mu_t \left[F\left[\frac{\partial \tilde{u}}{\partial y}\right]^2 + \left[\frac{\partial \tilde{w}}{\partial y}\right]^2 \right] \quad . \tag{51}$$

This shows that near y = 0 where $\frac{\partial \tilde{w}}{\partial y}$ may be large, the production term is strongly influenced by the non-isotropy. But experiments show that $\tilde{w}$, the cross flow velocity decreases very rapidly away from a spinning surface and for $y^+ > 5$

$$\tilde{w}^2 \cong 0.1\ \tilde{u}^2 \text{ and} \left[\frac{\partial \tilde{w}}{\partial y}\right]^2 \cong 0.01 \left[\frac{\partial \tilde{u}}{\partial y}\right]^2 \quad ,$$

so that for $y^+ > 5$

$$P \tilde{=} \mu_t \left[\left[\frac{\partial \tilde{u}}{\partial y}\right]^2 + F \left[\frac{\partial \tilde{w}}{\partial y}\right]^2 \right] \tilde{=} \mu_t \left[\frac{\partial \tilde{u}}{\partial y}\right]^2 \quad , \tag{52}$$

or essentially isotropic for the boundary layer situation. Because of the rapid fall off of the effect of spin on the cross flow velocity and the small cross flow velocities at small angles of attack, the non-isotropic effects can be expected to be very slight even for values of F significantly different from unity.

G. Algebraic Eddy Viscosity Models

Two forms of algebraic eddy viscosity were employed for comparison with the two-equation K-E model. For the boundary layer equations, a form of the Prandtl-van Driest mixing length approach was used

$$\mu_t = \bar{\rho}\, \ell^2 \left[\left|\frac{\partial \tilde{u}}{\partial y}\right| + \left|\frac{\partial \tilde{w}}{\partial y}\right| \right] \tag{53}$$

where

$$\ell/\delta = \lambda \tanh\left[\frac{\kappa y}{\lambda \delta}\right]\left[1 - \exp\left[-\frac{y^+}{A^+}\right]\right], \tag{54}$$

$$\lambda = 0.09, \ \kappa = 0.4, \ A^+ = 26.$$

The other model is the more sophisticated Baldwin-Lomax[21] technique, which was used in connection with the PNS code. This two layer model is based on the proportionality between μ_t and the local vorticity in the "innner" region, such that

$$(\mu_t)_{inner} = \bar{\rho}\, \ell^2 \, |\omega| \tag{55}$$

where

$$\ell = \kappa y \, [1 - \exp(-y^+/A^+)], \tag{56}$$

---

21. *Baldwin, B.S., and Lomax, H., "Thin Layer Approximation and Algebraic Model for Separated Turbulent Flows," AIAA Paper 78-257, January 1978.*

B. Boundary Layer Results

The results obtained with the Dwyer and Sanders boundary layer code incorporating the K-E turbulence model are fully described in van Gulick's thesis[11] and in a paper by van Gulick and Danberg.[12] Their results are only summarized here in regard to the comparison with the experimental data of Kayser and Sturek[22] and in regard to the effects of non-isotropy and buoyancy.

1. Experimental Data

Figure 3 shows the configuration tested in the Ballistic Research Laboratory wind tunnel by Kayser and Sturek. The tests were performed at M = 3.0, Reynolds number of 9.68×10^6 per meter and angles of attack of 0° and 2°. Measurements were made with and without the model spinning (Ω = 20,000 RPM). Wall pressure distributions were obtained for the non-spinning case and impact probe boundary layer surveys provided the major experimental results. The impact probe data were reduced to provide longitudinal velocity profiles assuming constant pressure across the boundary layer and employing a Crocco temperature-velocity relationship in lieu of measured temperature profiles. A number of stations were investigated but results will be limited to just one station at 3.33 caliber from the nose. This station is on the cylindrical mid-body just aft of the ogive-cylinder junction.

2. Comparison with Experimental Velocity Profiles

Figure 4 shows a typical set of velocity profiles at the X/D = 3.33 station. The experimental data are compared with the computed three-dimensional boundary layer code predictions using the algebraic and K-E turbulence models. The comparison is based on the physical variables and therefore demonstrates the ability of the computational system (inviscid and viscous flow) to predict the measured quantities. Displacement effects are, however, not included. The predicted velocities are generally less than those measured. The K-E prediction is in somewhat better agreement with the data than that of the algebraic model. The computed boundary layer thickness is larger than the experimental data which is in part caused by the incorrectly calculated pressure history obtained from the theoretical prediction. At $\phi = 180^0$, the lee side, the agreement is better at all stations investigated and the lee side experimental data are expected to be more reliable because of the thickness of the profile.

A comparison is also shown in Figure 5 between the experimental profile data and prediction based on non-dimensionalized variables. The local velocity is normalized by the boundary layer edge velocity and the normal

---

22. *Kayser, L.D., and Sturek, W.B., "Experimental Measurements in the Turbulent Boundary Layer of a Yawed, Spinning Ogive-Cylinder Body of Revolution at Mach 3.0. Part II: Data Tabulation," US Army Ballistic Research Laboratory, Memorandum Report ARBRL-MR-02813, March 1978.*

distance by the boundary layer edge velocity and the normal distance by the boundary layer thickness. This presentation concentrates on the ability of the prediction to reproduce the form of the turbulent profile independent of any discrepancy in the outer boundary condition. The results show that the K-E method is generally superior to the algebraic solution although the algebraic solution is at most 7 percent lower than the K-E solution.

Figures 6 and 7 show typical $\tilde{K}$ and $\tilde{E}$ profiles close to the wall obtained from these calculations. These results are non-dimensionalized in terms of law-of-the-wall variables

$$(K^+ = \tilde{K}/u_\tau^2,\ E^+ = \nu_w \tilde{E}/u_\tau^4,\ y^+ = u_\tau y/\nu_w,\ \text{where } u_\tau = (\tau_w/\rho)^{1/2}).$$

3. Effect of Non-Isotropy

Rotta's non-isotropy formulation of the turbulent stresses was incorporated into the boundary layer mean flow equations. The K-E or algebraic turbulence model provided the μ_t which is multiplied by an effective velocity gradient composed of an isotropic and non-isotropic part

$$\left[\frac{d\tilde{u}}{dy}\right]_{\substack{\text{effective}\\ \text{Isotropic}}} = \frac{\partial \tilde{u}}{\partial y} - (1-F)\underbrace{\left[\frac{\partial \tilde{u}}{\partial y} - \frac{\tilde{u}\left[\tilde{u}\frac{\partial \tilde{u}}{\partial y} + \tilde{w}\frac{\partial \tilde{w}}{\partial y}\right]}{(\tilde{u}^2 + \tilde{w}^2)}\right]}_{\text{Non-Isotropic}}. \qquad (65)$$

Figure 8 shows a plot of the isotropic and non-isotropic terms for a typical solution. The non-isotropic part is seen to fall off dramatically. The net effect on the longitudinal flow is found to be small for all the conditions considered. In varying the constant F between 1 and 0.25, the u-velocity profiles and longitudinal c_{f_x} do not change discernably (see Figure 9). However, the circumferential flow is significantly affected as shown in Figure 10 where the circumferential skin friction coefficient is plotted against angular position for the spinning body. The general effect of decreasing F is to increase nearly linearly and uniformly the circumferential friction (in this case to decrease the calculated roll damping). The longitudinal skin friction decreases slightly because of this formulation of the shear stresses. This implies an exchange of momentum from longitudinal to the circumferential direction with decreasing F consistent with the assumptions underlying Rotta's stress tensor.

4. Effects of Streamline Curvature

Bradshaw[23] has proposed an effect of streamline curvature on turbulence based on an analogy with buoyancy effects. Bradshaw's proposal called for a modification of the mixing length by a linear factor involving the turbulent Richardson number.

The fundamental interpretation of Richardson number is that of a ratio of buoyancy to inertia forces.[24] For example, Reference 6 cites a formulation by Prandtl, as:

$$Ri = -g\left[\frac{1}{\rho}\frac{\partial \rho}{\partial y}\right] \Big/ \left[\frac{\partial u}{\partial y}\right]^2 \quad . \tag{66}$$

Bradshaw has shown that this can be interpreted as the ratio of two time scales squared. He then defined a time scale for the mean flow for curved streamlines as

$$(\text{mean flow time scale})^2 = \left\{\frac{V_\theta^2}{r}\left[\frac{1}{rV_\theta}\frac{\partial (rV_\theta)}{\partial y}\right]\right\}^{-1}$$

where V_θ^2/r is the radial acceleration and the term in the square brackets is the inverse of a length scale based on the rate of change of angular momentum. He compared this to a time scale for turbulence

$$(\text{turbulent time scale})^2 = \left(\frac{\ell}{\sqrt{\overline{u'^2}}}\right)^2 \simeq \frac{\ell^2}{\ell^2\left[\frac{\partial V_\theta}{\partial y}\right]^2} \quad .$$

Thus the Richardson number for turbulent flow along curved streamlines is defined

$$Ri_t = \frac{V_\theta^2}{r^2}\frac{\partial (rV_\theta)}{\partial y} \Big/ \left[\frac{\partial V_\theta}{\partial y}\right]^2 \quad .$$

Bradshaw also noted that compressibility would effect the turbulent Richardson number and he recommended it increase in proportion to $(1 + \frac{\gamma-1}{2} M^2)$.

---

23. *Bradshaw, P., "The Analogy Between Streamline Curvature and Buoyancy in Turbulent Shear Flow," J. Fluid Mech., Vol. 36, Part I, 1969.*

24. *Arpaci, V.S., and Larsen, P.S., "Convective Heat Transfer," Prentice-Hall, 1984.*

Launder et al[25] have attempted to extend these ideas to the K-E theory by redefining the turbulent time scale as $\tilde{K}/\tilde{E}$ so that

$$Ri_t = \left[(\tilde{K}V_\theta)^2 \frac{\partial(rV_\theta)}{\partial y} \Big/ (r\tilde{E})^2 \right] (1 + \frac{\gamma-1}{2} M^2) . \qquad (68)$$

It was suggested that the most appropriate way for the Richardson number to influence the Reynolds stresses was through modification of one or more of the empirical constants in the $\tilde{E}$ equation. Specifically it was recommended that C_2 be increased by the factor

$$1 - C_c Ri_t \qquad (69)$$

where a value of $C_c = 0.2$ was cited as optimum based on results for low speed rotating body flow fields.

Calculations were made for the wind tunnel configuration previously described at 2° angle of attack and with spin. The Richardson number was estimated locally in terms of the circumferential velocity, $\tilde{w}$, because it was anticipated that the major effect would be associated with the circumferential flow near the model surface. The Ri_t employed was

$$Ri_t = 2 \frac{\tilde{K}^2}{\tilde{E}^2} \frac{\tilde{w}}{r^2} \left[\frac{\partial r\tilde{w}}{\partial y} \right] (1 + \frac{\gamma-1}{2} M^2) . \qquad (70)$$

This modification of the dissipation in the $\tilde{E}$ equation had very little effect. The longitudinal skin friction was slightly increased as shown in Figure 11. The magnitude of the streamline curvature effect is negligible for the present situation. This result might be different at higher angles of attack.

IV. APPLICATION TO THE PARABOLIZED NAVIER-STOKES CODE

A. Mean-Flow Equations

The parabolized Navier-Stokes method (PNS) employed here was developed by Schiff and Steger[2] as a technique for calculating steady, supersonic, high Reynolds number flow about three-dimensional configurations with moderate axial geometry variation. The PNS equations are obtained from equations (12), (13) and (30) which can be written in the following compact form:

---

25. *Launder, B.E., Priddin, C.H., and Sharma, B.F., "The Calculation of Turbulent Boundary Layers on Spinning and Curved Surfaces," J. Fluids Engineering, pp. 231-239, March 1977.*

$$\frac{\partial E}{\partial x} + \frac{\partial F}{\partial y} + \frac{\partial G}{\partial z} = Re^{-1} \left[\frac{\partial R}{\partial x} + \frac{\partial S}{\partial y} + \frac{\partial W}{\partial z} \right] \tag{71}$$

where

$$E = \begin{bmatrix} \bar{\rho}\tilde{u} \\ \bar{\rho}\tilde{u}^2 + \bar{p} \\ \bar{\rho}\,\tilde{u}\,\tilde{v} \\ \bar{\rho}\,\tilde{u}\,\tilde{w} \\ (\bar{e} + \bar{p})\,\tilde{u} \end{bmatrix} \qquad F = \begin{bmatrix} \bar{\rho}\,\tilde{v} \\ \bar{\rho}\,\tilde{v}\,\tilde{u} \\ \bar{\rho}\,\tilde{v}^2 + \bar{p} \\ \bar{\rho}\,\tilde{v}\,\tilde{w} \\ (\bar{e} + \bar{p})\,\tilde{v} \end{bmatrix}$$

$$G = \begin{bmatrix} \bar{\rho}\,\tilde{w} \\ \bar{\rho}\,\tilde{u}\,\tilde{w} \\ \bar{\rho}\,\tilde{v}\,\tilde{w} \\ \bar{\rho}\,\tilde{w}^2 + \bar{p} \\ (\bar{e} + \bar{p})\,\tilde{w} \end{bmatrix} \qquad q = \begin{bmatrix} \bar{\rho} \\ \bar{\rho}\,\tilde{u} \\ \bar{\rho}\,\tilde{v} \\ \bar{\rho}\,\tilde{w} \\ \bar{e} \end{bmatrix}$$

$$P = \begin{bmatrix} 0 \\ \tau_{xx} \\ \tau_{yx} \\ \tau_{zx} \\ R_5 \end{bmatrix} \qquad S = \begin{bmatrix} 0 \\ \tau_{xy} \\ \tau_{yy} \\ \tau_{zy} \\ S_5 \end{bmatrix} \qquad W = \begin{bmatrix} 0 \\ \tau_{xz} \\ \tau_{yz} \\ \tau_{zz} \\ W_5 \end{bmatrix}$$

$$\tau_{ij} = (\bar{\mu}+\mu_t)\tilde{d}_{ij} = (\bar{\mu}+\mu_t)\left[\frac{\partial \tilde{u}_i}{\partial x_j} + \frac{\partial \tilde{u}_j}{\partial x_i} - \frac{2}{3}\frac{\partial \tilde{u}_k}{\partial x_k}\delta_{ij} \right]$$

$$R_5 = \tilde{u}\tau_{xx} + \tilde{v}\tau_{xy} + \tilde{w}\tau_{xz} + \frac{1}{(\gamma-1)}\left[\frac{\bar{\mu}}{Pr} + \frac{\mu_t}{Pr_t} \right] \frac{\partial \overline{a^2}}{\partial x}$$

$$S_5 = \tilde{u}\tau_{yx} + \tilde{v}\tau_{yy} + \tilde{w}\tau_{yz} + \frac{1}{(\gamma-1)}\left[\frac{\bar{\mu}}{Pr} + \frac{\mu_t}{Pr_t}\right]\frac{\partial \overline{a^2}}{\partial y}$$

$$W_5 = \tilde{u}\tau_{zx} + \tilde{v}\tau_{zy} + \tilde{w}\tau_{zz} + \frac{1}{(\gamma-1)}\left[\frac{\bar{\mu}}{Pr} + \frac{\mu_t}{Pr_t}\right]\frac{\partial \overline{a^2}}{\partial z}$$

The physical x, y, z Cartesian coordinate system is transformed into new body oriented computational coordinates ξ, η, ζ as illustrated in Figure 12. This transformation simplifies the application of boundary conditions and makes it possible to neglect certain viscous terms because of the high Reynolds number - thin shear layer approximation.[2 26] The transformation relations are:

$$\xi = \xi(x) \qquad \text{Jacobian} = J$$

$$\eta = \eta(x,y,z) \qquad J = x_\xi^{-1}(y_\eta z_\zeta - y_\zeta z_\eta) \ .$$

$$\zeta = \zeta(x,y,z)$$

The resulting PNS equations become:

$$\frac{\partial \vec{E}}{\partial \xi} + \frac{\partial \vec{F}}{\partial \eta} + \frac{\partial \vec{G}}{\partial \zeta} = Re^{-1}\frac{\partial \vec{S}}{\partial \zeta} \ , \tag{72}$$

$$\vec{E} = J^{-1}\begin{bmatrix} \bar{\rho}\,U \\ \bar{\rho}\,\tilde{u}\,U + \xi_x\,\bar{p} \\ \bar{\rho}\,\tilde{v}\,U \\ \bar{\rho}\,\tilde{w}\,U \\ (\bar{e} + \bar{p})\,U \end{bmatrix} \qquad \vec{F} = J^{-1}\begin{bmatrix} \bar{\rho}\,V \\ \bar{\rho}\,\tilde{u}\,V + \eta_x\,\bar{p} \\ \bar{\rho}\,\tilde{v}\,V + \eta_\eta\,\bar{p} \\ \bar{\rho}\,\tilde{w}\,V + \eta_z\,\bar{p} \\ (\bar{e} + \bar{p})\,V \end{bmatrix},$$

$$\vec{G} = J^{-1}\begin{bmatrix} \bar{\rho}\,W \\ \bar{\rho}\,\tilde{u}\,W + \zeta_x\,\bar{p} \\ \bar{\rho}\,\tilde{v}\,W + \zeta_y\,\bar{p} \\ \bar{\rho}\,\tilde{w}\,W + \zeta_z\,\bar{p} \\ (\bar{e} + \bar{p})\,W \end{bmatrix} \qquad \vec{q} = J^{-1}\begin{bmatrix} \bar{\rho} \\ \bar{\rho}\,\tilde{u} \\ \bar{\rho}\,\tilde{v} \\ \bar{\rho}\,\tilde{w} \\ \bar{e} \end{bmatrix} \ .$$

---

26. *Steger, J.L., "Implicit Finite-Difference Simulation of Flow About Arbitrary Two-Dimensional Geometries,"* AIAA Journal, *Vol. 16, No. 7, July 1978.*

These equations have the strong conservation form while retaining the Cartesian velocity components as dependent variables. The contravariant velocity components U, V, W are defined as:

$$U = \xi_x \tilde{u}$$

$$V = \eta_x \tilde{u} + \eta_y \tilde{v} + \eta_z \tilde{w} \qquad (73)$$

$$W = \zeta_x \tilde{u} + \zeta_y \tilde{v} + \zeta_z \tilde{w} .$$

The thin viscous layer approximation retains only those terms involving derivatives with respect to ζ, the near normal to the wall coordinate. Thus the RHS terms can be written as:

$$\hat{S} = J^{-1} \begin{bmatrix} 0 \\ (\bar{\mu}+\mu_t)\left[(\zeta_x^2+\zeta_y^2+\zeta_z^2)\tilde{u}_\zeta + \frac{1}{3}(\zeta_x\tilde{u}_\zeta+\zeta_y\tilde{v}_\zeta+\zeta_z\tilde{w}_\zeta)\zeta_x\right] \\ (\bar{\mu}+\mu_t)\left[(\zeta_x^2+\zeta_y^2+\zeta_z^2)\tilde{v}_\zeta + \frac{1}{3}(\zeta_x\tilde{u}_\zeta+\zeta_y\tilde{v}_\zeta+\zeta_z\tilde{w}_\zeta)\zeta_y\right] \\ (\bar{\mu}+\mu_t)\left[(\zeta_x^2+\zeta_y^2+\zeta_z^2)\tilde{w}_\zeta + \frac{1}{3}(\zeta_x\tilde{u}_\zeta+\zeta_y\tilde{v}_\zeta+\zeta_z\tilde{w}_\zeta)\zeta_z\right] \\ (\bar{\mu}+\mu_t)\left[(\zeta_x^2+\zeta_y^2+\zeta_z^2)\left(\tilde{u}^2+\tilde{v}^2+\tilde{w}^2\right)_\zeta \right. \\ \qquad \left. + \frac{1}{3}(\zeta_x\tilde{u}+\zeta_y\tilde{v}+\zeta_z\tilde{w})\left(\zeta_x\tilde{u}_\zeta+\zeta_y\tilde{v}_\zeta+\zeta_z\tilde{w}_\zeta\right)\right] \\ \qquad + \frac{1}{(\gamma-1)}\left(\frac{\bar{\mu}}{Pr}+\frac{\mu_t}{Pr_t}\right)\frac{\partial \overline{a^2}}{\partial \zeta} \end{bmatrix} .$$

The numerical integration scheme used is the implicit approximate factorized algorithm in delta form developed by Beam and Warming.[3 27] The

---

27. *Beam, R.M., and Warming, R.F., "An Implicit Factored Scheme for the Compressible Navier-Stokes Equations," AIAA J., Vol. 16, No. 4, April 1978.*

difference equations are linearized in their vector form and the solution requires block tridiagonal inversion at each marching step. See reference 28 for additional details and applications.

B. Turbulence Models

The Baldwin-Lomax algebraic model[21] was incorporated into the method as it appears in the work of Schiff and Sturek.[29] The K-E equations (38) and (39) were incorporated by Kim[13] in the steady, supersonic PNS code paralleling the work of Sahu[14] in his application of the $\tilde{K}$-$\tilde{E}$ equations to the time-dependent, transonic Navier-Stokes problem. A new formulation of the turbulent viscosity subroutine from that employed by van Gulick was required because of the body oriented coordinate transformations in the PNS solution. The $\tilde{K}$-$\tilde{E}$ equations can be written in a transformed form similar to the mean flow equations, i.e.:

$$\frac{\partial \vec{A}}{\partial \xi} + \frac{\partial \vec{B}}{\partial \eta} + \frac{\partial \vec{C}}{\partial \zeta} = Re^{-1} \frac{\partial \vec{D}}{\partial \zeta} + \vec{H} \ , \tag{74}$$

where

$$\vec{A} = J^{-1} \begin{bmatrix} \bar{\rho}\,\tilde{K}\,U \\ \bar{\rho}\,\tilde{E}\,U \end{bmatrix} \ ; \qquad \vec{B} = J^{-1} \begin{bmatrix} \bar{\rho}\,\tilde{K}\,V \\ \bar{\rho}\,\tilde{E}\,V \end{bmatrix} \ ;$$

$$\vec{C} = J^{-1} \begin{bmatrix} \bar{\rho}\,\tilde{K}\,W \\ \bar{\rho}\,\tilde{E}\,W \end{bmatrix} ; \qquad \vec{D} = J^{-1} \begin{bmatrix} \left[\frac{\mu_t}{\sigma_K} + \bar{\mu}\right](\zeta_x^2+\zeta_y^2+\zeta_z^2)\tilde{K}_\zeta \\ \left[\frac{\mu_t}{\sigma_E} + \bar{\mu}\right](\zeta_x^2+\zeta_y^2+\zeta_z^2)\tilde{E}_\zeta \end{bmatrix} \ ;$$

$$\vec{q} = J^{-1} \begin{bmatrix} \bar{\rho}\,\tilde{K} \\ \bar{\rho}\,\tilde{E} \end{bmatrix} \ ;$$

---

28. *Sturek, W.B., and Schiff, L.B., "Computation of the Magnus Effect for Slender Bodies in Supersonic Flow," AIAA Paper 80-1586CP, August 1980.*

29. *Schiff, L.B., and Sturek, W.B., "Numerical Simulation of Steady Supersonic Flow Over an Ogive-Cylinder-Boattail Body," AIAA Paper 80-0066, January 1980.*

$$\hat{H} = J^{-1} \begin{bmatrix} \frac{\mu_t}{Re}\left[(\zeta_x^2+\zeta_y^2+\zeta_z^2)(\tilde{u}_\zeta^2+\tilde{v}_\zeta^2+\tilde{w}_\zeta^2) + (\tilde{u}_\zeta\zeta_x+\tilde{v}_\zeta\zeta_y+\tilde{w}_\zeta\zeta_z)^2\right] \\ - \frac{c_\mu \bar{\rho}^2 \tilde{K}^2 Re}{\mu_t} - \frac{2\bar{\mu}\tilde{K}}{Re\, y_n^2} \\ C_1\left[\frac{\tilde{E} c_\mu \bar{\rho} \mu_t}{Re}\right]^{1/2}\left[(\zeta_x^2+\zeta_y^2+\zeta_z^2)(\tilde{u}_\zeta^2+\tilde{v}_\zeta^2+\tilde{w}_\zeta^2)\right. \\ \left. + (\tilde{u}_\zeta\zeta_x+\tilde{v}_\zeta\zeta_y+\tilde{w}_\zeta\zeta_z)^2\right] - c_2(\bar{\rho}\tilde{E})^{3/2}\left[\frac{c_\mu Re}{\mu_t}\right]^{1/2} \\ - \frac{2\bar{\mu}\tilde{E}}{y_n^2 Re}\exp(-y_n^+/2) \end{bmatrix}$$

Note: these equations have been non-dimensionalized using a_∞, ρ_∞, μ_∞ (free-stream properties) and the body reference diameter D. Thus the Reynolds number parameter is:

$$Re = \rho_\infty a_\infty D/\mu_\infty \, . \tag{75}$$

In addition, $\tilde{E}$ has been eliminated from the $\tilde{K}$ equation and $\tilde{K}$ from the $\tilde{E}$-equation using the following definition of the turbulent viscosity

$$\mu_t = Re\, c_\mu\, \bar{\rho}\, \tilde{K}^2/\tilde{E} \, . \tag{76}$$

Thus the equations are decoupled but require an estimate of μ_t.

1. Finite Difference Approximation

The governing $\tilde{K}$-$\tilde{E}$ equations have a form similar to that of the mean flow PNS equations. In fact they could be solved by increasing the order of the block tridiagonal inversion scheme of the PNS code but this would have reduced the flexibility of the code and increased the running time. The same kind of linearization and implicit factorized delta form is employed for the $\tilde{K}$-$\tilde{E}$ equation with the exception that in the decoupled form the inversion requires only an efficient tridiagonal algorithm. The boundary conditions employed at the body surface are the same as in the boundary layer case, i.e., $\tilde{K} = \tilde{E} = 0$. At the outer boundary a zero gradient condition was applied

$$\frac{\partial \tilde{K}}{\partial \zeta} = \frac{\partial \tilde{E}}{\partial \zeta} = 0 \ .$$

Thus questions regarding the determination of the edge of the boundary layer and evaluation of the inviscid $\tilde{K}$-$\tilde{E}$ equations along an inviscid streamline were avoided. The above conditions were applied at an arbitrary point well away from the viscous layer near the body.

The initial conditions employed to start the calculation are based on equating the production and dissipation terms. This is obviously incorrect at the wall and at the outer edge of the boundary layer. However, the error is expected to decay as the flow develops. The resulting equations for initial values of $\tilde{K}$ and $\tilde{E}$ are

$$\tilde{K} = \frac{\mu_t}{\sqrt{Re}\ \bar{\rho}\ \sqrt{c_\mu}} \left[(\zeta_x^2+\zeta_y^2+\zeta_z^2)\ (\tilde{u}_\zeta^2+\tilde{v}_\zeta^2+\tilde{w}_\zeta^2) + (\tilde{u}_\zeta\zeta_x+\tilde{v}_\zeta\zeta_y+\tilde{w}_\zeta\zeta_z)^2\right]^{1/2}$$

$$\tilde{E} = \frac{\mu_t}{\bar{\rho}\ Re} \left[(\zeta_x^2+\zeta_y^2+\zeta_z^2)\ (\tilde{u}_\zeta^2+\tilde{v}_\zeta^2+\tilde{w}_\zeta^2) + (\tilde{u}_\zeta\zeta_x+\tilde{v}_\zeta\zeta_y+\tilde{w}_\zeta\zeta_z)^2\right]. \qquad (77)$$

The turbulent viscosity and initial velocity distribution were obtained using the algebraic model ahead of the station where the $\tilde{K}$-$\tilde{E}$ equations were first introduced. A more complete description of the finite difference procedure can be found in Kim's Thesis.[13]

C. Preliminary Results Using K-E Model in the PNS Code

The experimental data from the ogive-cylinder-boattail projectile configuration were used to evaluate the PNS Code. The calculations, however, were limited to zero angle of attack and zero spin. The code was run on the University of Delaware computer system and required 45 minutes of CPU time to complete just 160 steps. Because of the long running time on this system only a few runs were made in an attempt to verify the program.

Figure 13 shows one of the velocity profiles obtained at the X/D = 3.33 station. The difference between the K-E and algebraic computation is not significant at this point. The agreement with the experimental data is not significantly different from that of the boundary layer solution despite the fact that the PNS calculation included the inviscid as well as the viscous flow field. The close agreement between the two turbulent viscosity models is shown in Figure 14 where both methods give essentially identical results out to a y^+ of 100 near the maximum in μ_t. Beyond that point, the K-E turbulent viscosity falls off more rapidly than the algebraic theory but the difference has little effect on the computed velocity profile. The $\tilde{K}$ and $\tilde{E}$ profiles on which the μ_t values are based are shown in Figures 15 and 16. These show unexpected sharp peaks and lack of profile structure. It is believed that further computational experimentation is needed to provide additional substantiation and extend these results.

V. CONCLUDING REMARKS

A two-equation model of turbulence based on equations for the turbulent kinetic energy and energy dissipation has been formulated and applied to the solution of supersonic, three-dimensional flow and the results compared to experimental data. Two solution techniques were studied; the boundary layer theory approach and the parabolized Navier-Stokes method.

The boundary layer calculations were made using the K-E turbulence model and compared to results employing an algebraic turbulent viscosity model. Both turbulence models gave good agreement with velocity profiles obtained on a spinning ogive-cylinder-boattail configuration. The K-E model gave slightly better results regarding the shape of the profile but both numerical predictions over-estimated the boundary layer thickness.

The parabolized Navier-Stokes technique has the advantage of computing the entire flow field at one time including the viscous and inviscid regions. In order to make the K-E turbulence model compatible with the PNS method, the turbulence equation had to be reformulated in body oriented curvilinear coordinates. Preliminary results with this code also showed good agreement when compared to an algebraic turbulence model and with experimental velocity profile data.

The fundamental assumptions inherent in the compressible, turbulent flow equations were reviewed. The formulation is based on mass-weighted time averaged variables, although no distinction was made between mass-weighted time average and the measured average velocity of the experimental data. In developing the final form of the conservation equations it is necessary to neglect fluctuations in molecular thermal conductivity and viscosity and other terms in the momentum and energy equations that arise because of the kind of averaging employed. The effects of these assumptions are hidden within the subsequent modeling approximations made to achieve closure. Progress in developing a fully consistent system of equations will require consideration of the importance of the neglected terms.

An assumption that has also been made in the compressible flow equations, is that the total energy consists of only the thermodynamic internal energy and kinetic energy of the mean flow. The kinetic energy of the turbulent motion may be expected to be important close to any surface and thus have an important effect on the mean pressure as well as temperature in that region.

The effect of incorporating Rotta's non-isotropic theory for the Reynolds stresses was investigated using the boundary layer formulation. Even for widely varying values of the independent parameter of that theory, relatively little effect on the final solution was observed. The cross flow variable $c_{f\phi}$ and cross flow velocity were most significantly effected indicating an exchange of momentum from the longitudinal to the circumferential flow. The test case was for small angles of attack with small non-isotropic Reynolds stresses and the corresponding effect on the dissipation term in the K-E equation may be important.

Bradshaw's streamline curvature theory was also studied in the boundary layer. The Richardson number effect on the dissipation equation had essentially no effect on the overall solution for the spinning body in the supersonic flow investigated.

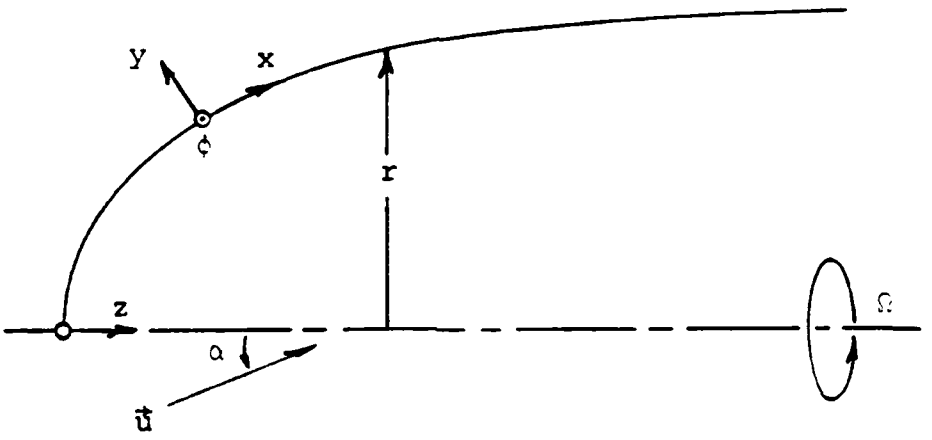

Figure 1. Boundary Layer Coordinate System

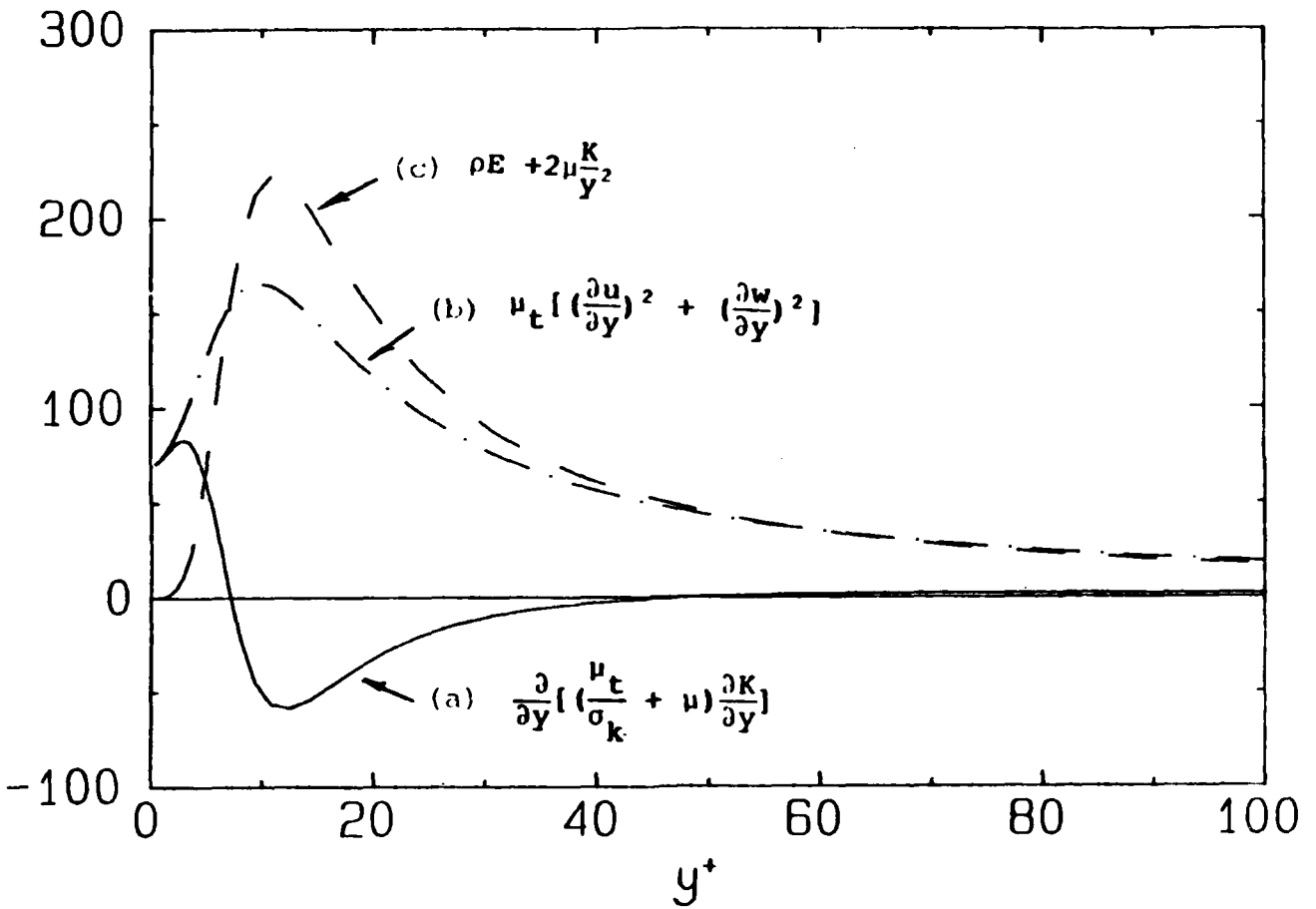

Figure 2. Terms in the Turbulent Kinetic Energy Equation (Diffusion, Production, Dissipation)

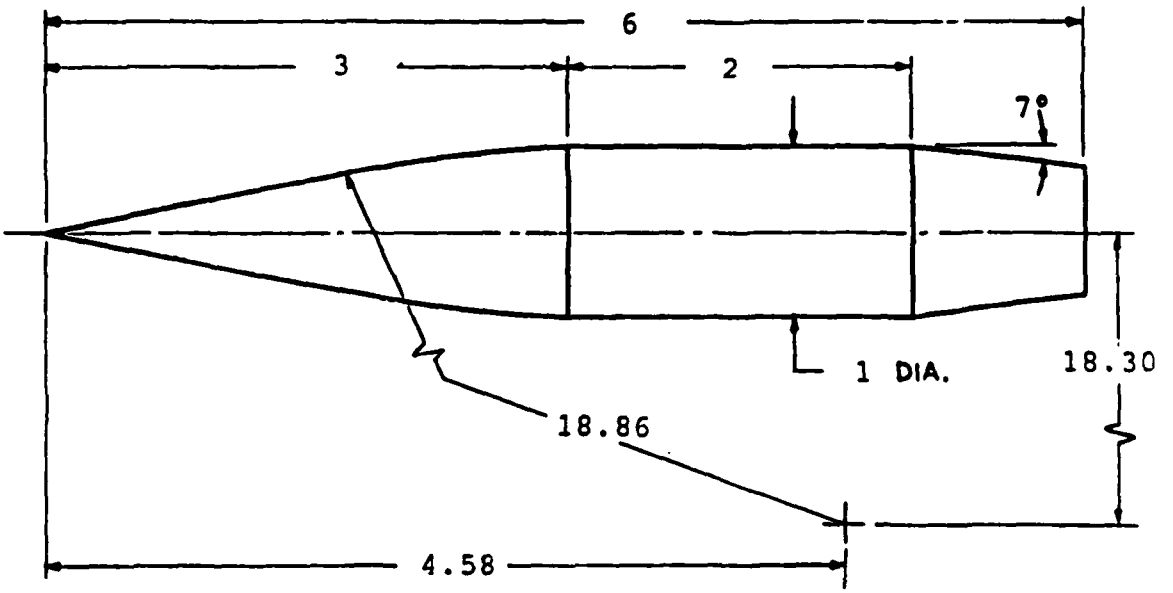

NOTE: DIMENSIONS ARE IN CALIBERS

Figure 3. Axisymmetric Configuration

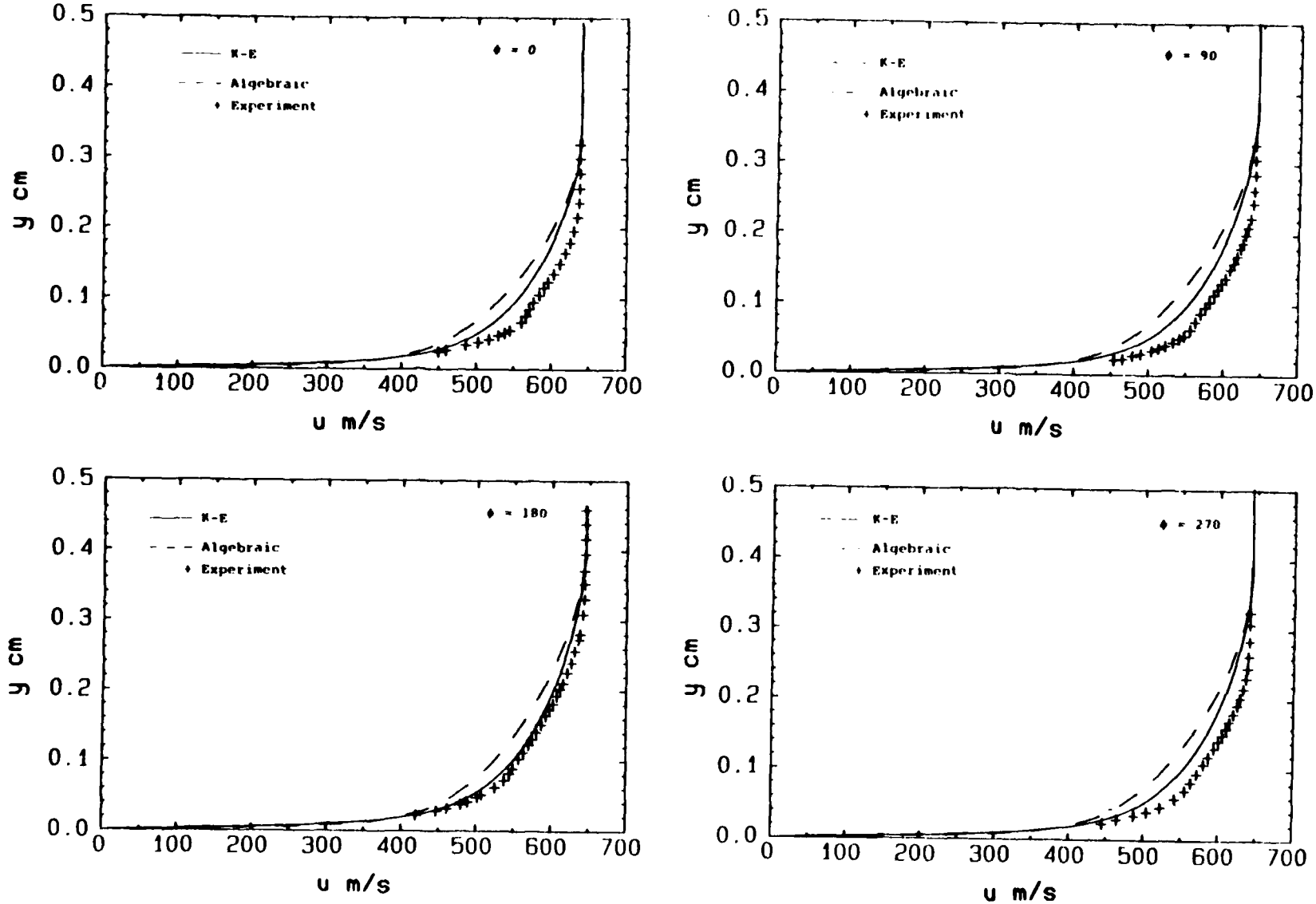

Figure 4. Boundary Layer U Velocity Component (X/D = 3.33)

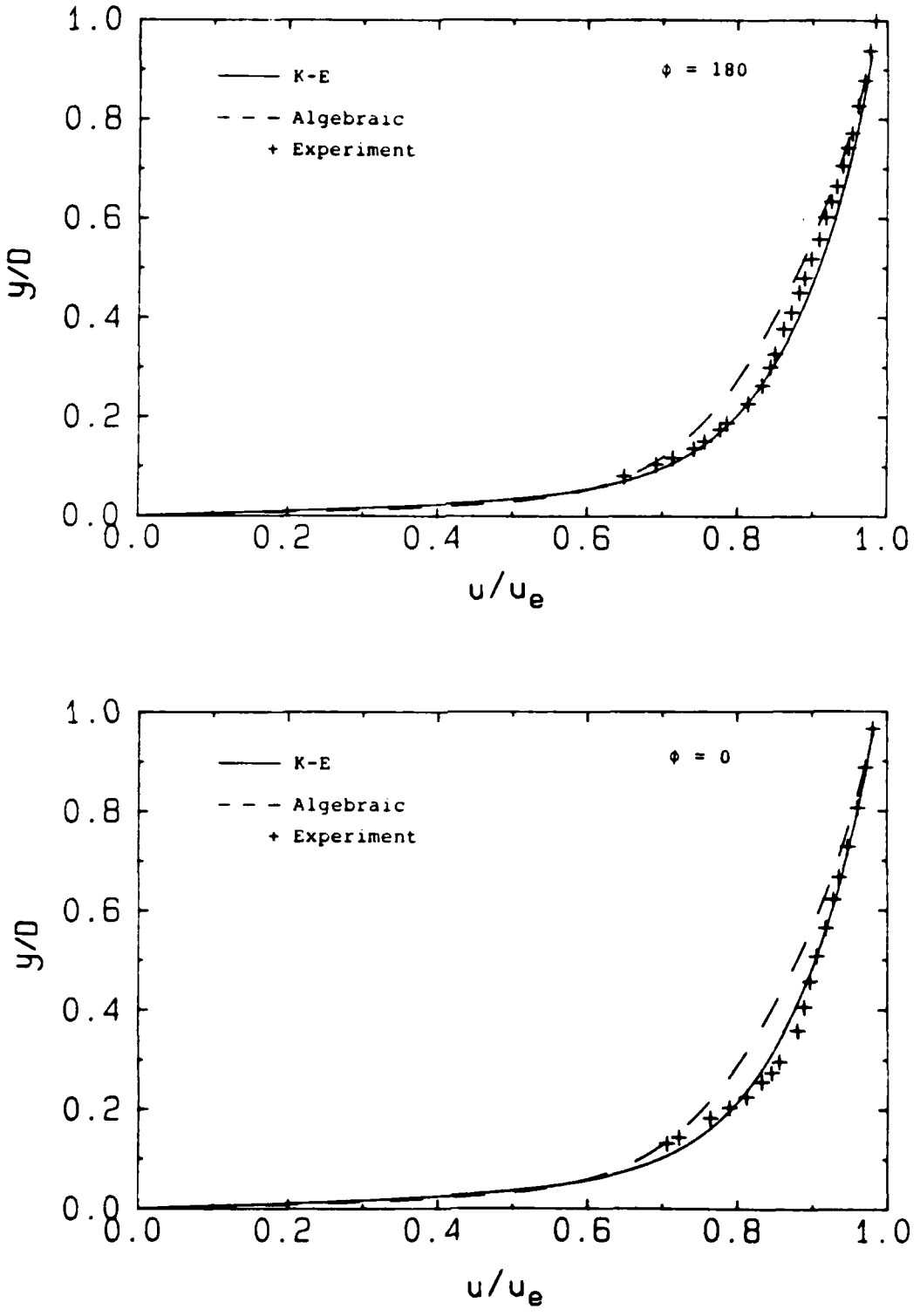

Figure 5. Boundary Layer Non-Dimensional Velocity Profiles

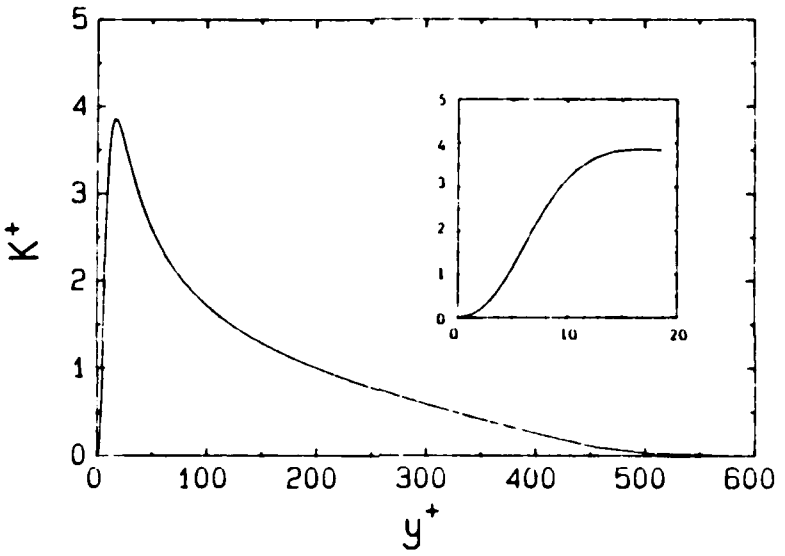

Figure 6. K^+ versus y^+ of the Boundary Layer Solution

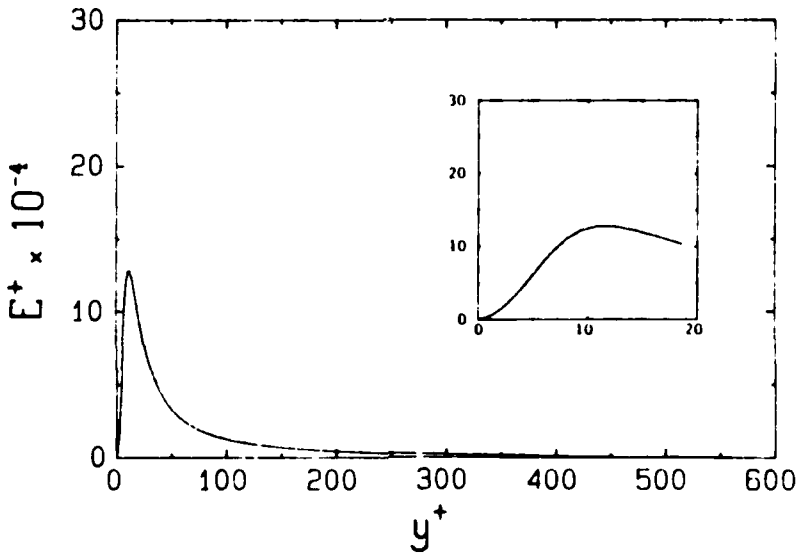

Figure 7. E^+ versus y^+ of the Boundary Layer Solution

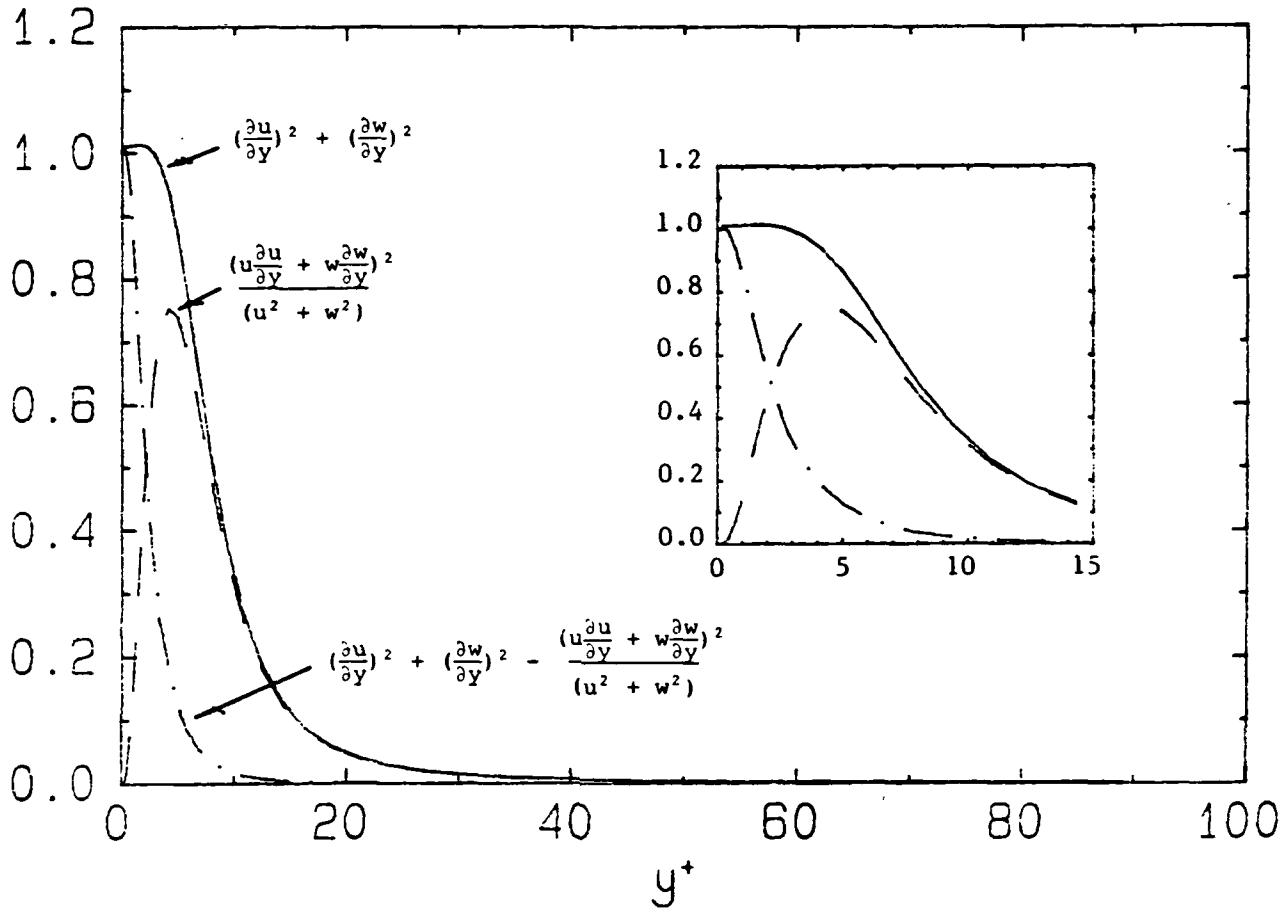

Figure 8. Isotropic and Non-Isotropic Contribution to the Turbulent Shear Stress

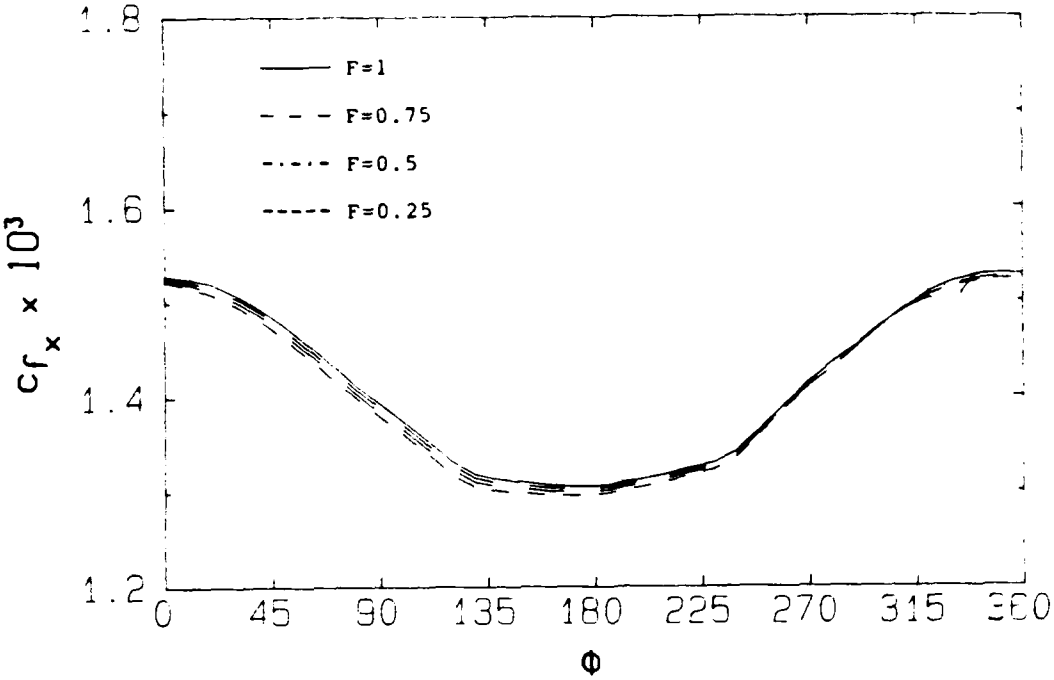

Figure 9. Effect of the Non-Isotropic Parameter F on the Longitudinal Skin Friction Coefficient

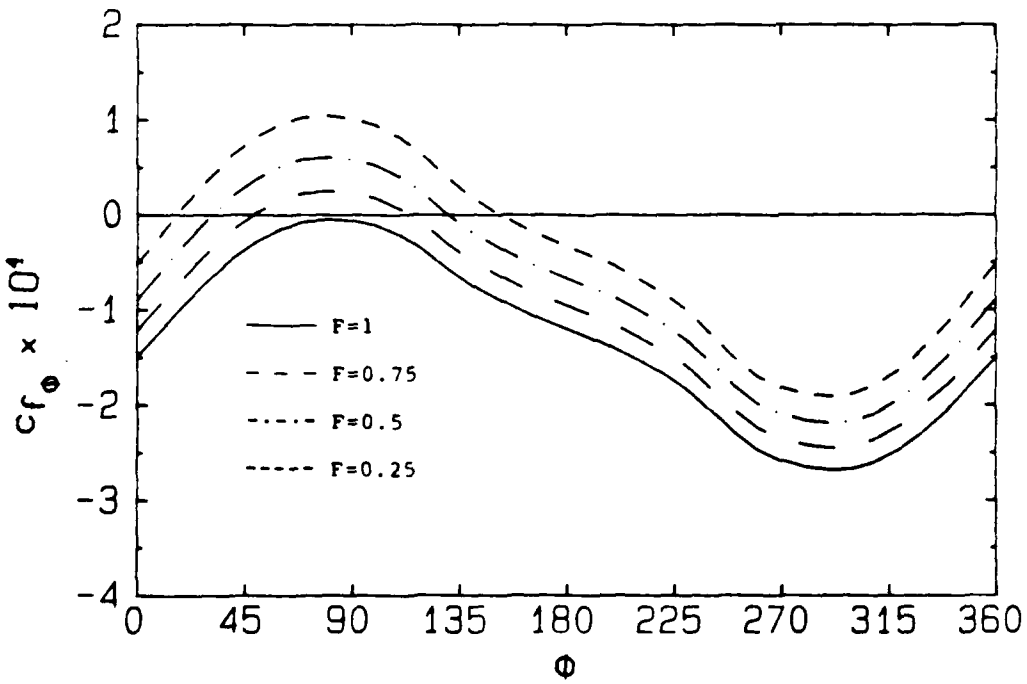

Figure 10. Effect of the Non-Isotropic Parameter F on Circumferential Skin Friction Coefficient

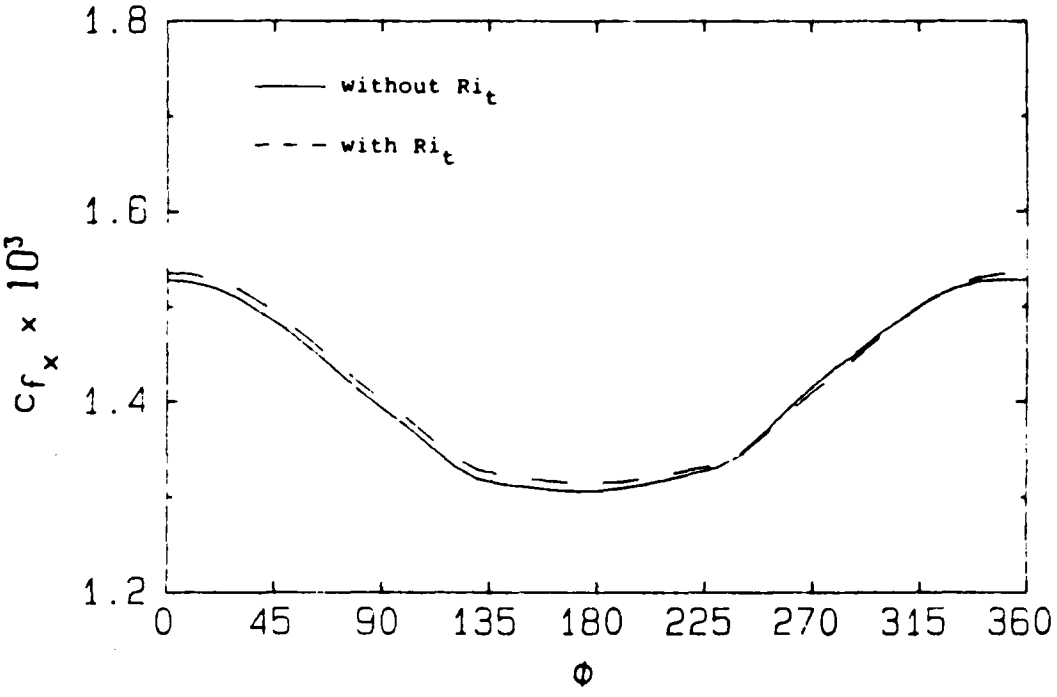

Figure 11. Effect of Streamline Curvature on Longitudinal Skin Friction Coefficient

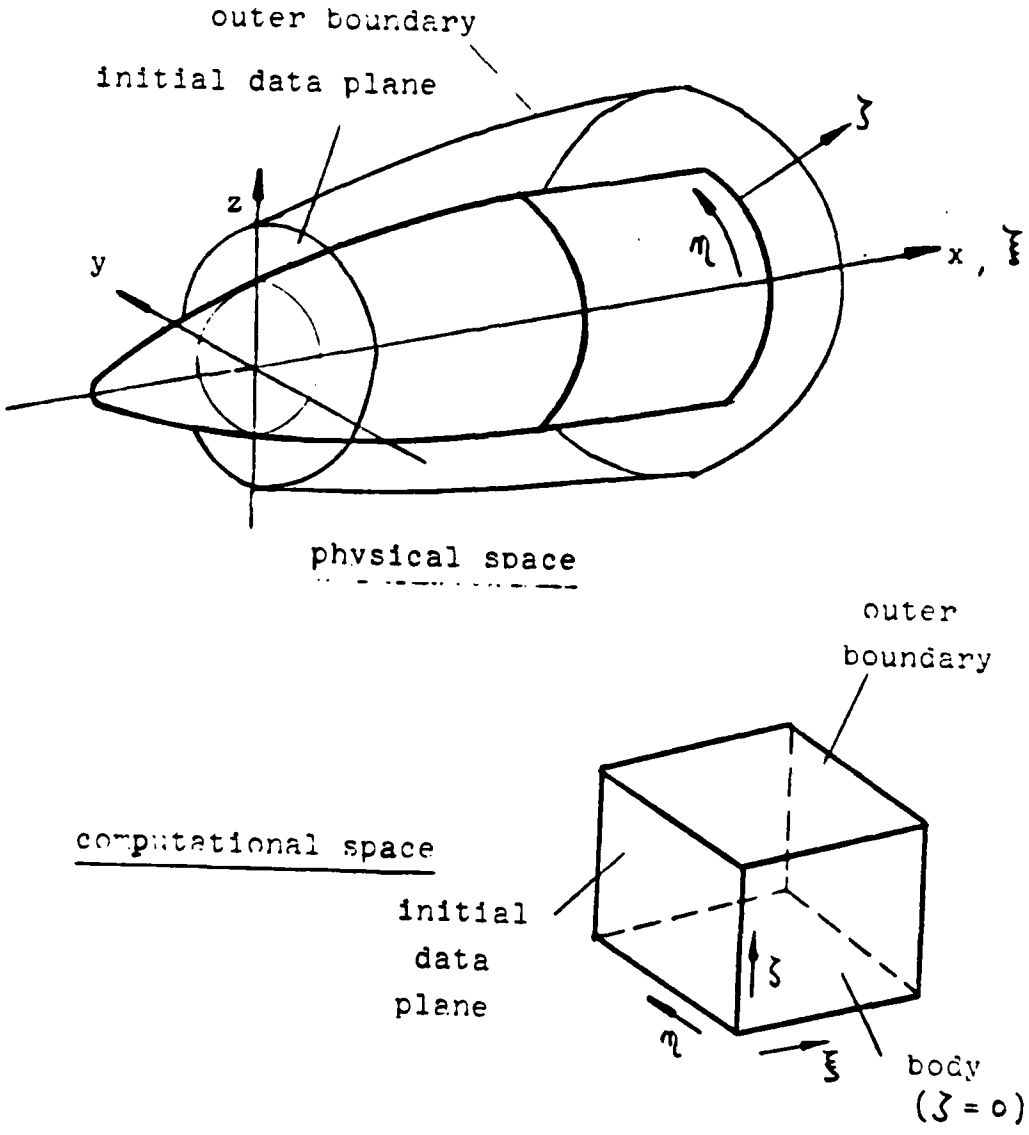

Figure 12. Transformation of Physical Coordinates into Computational Coordinates

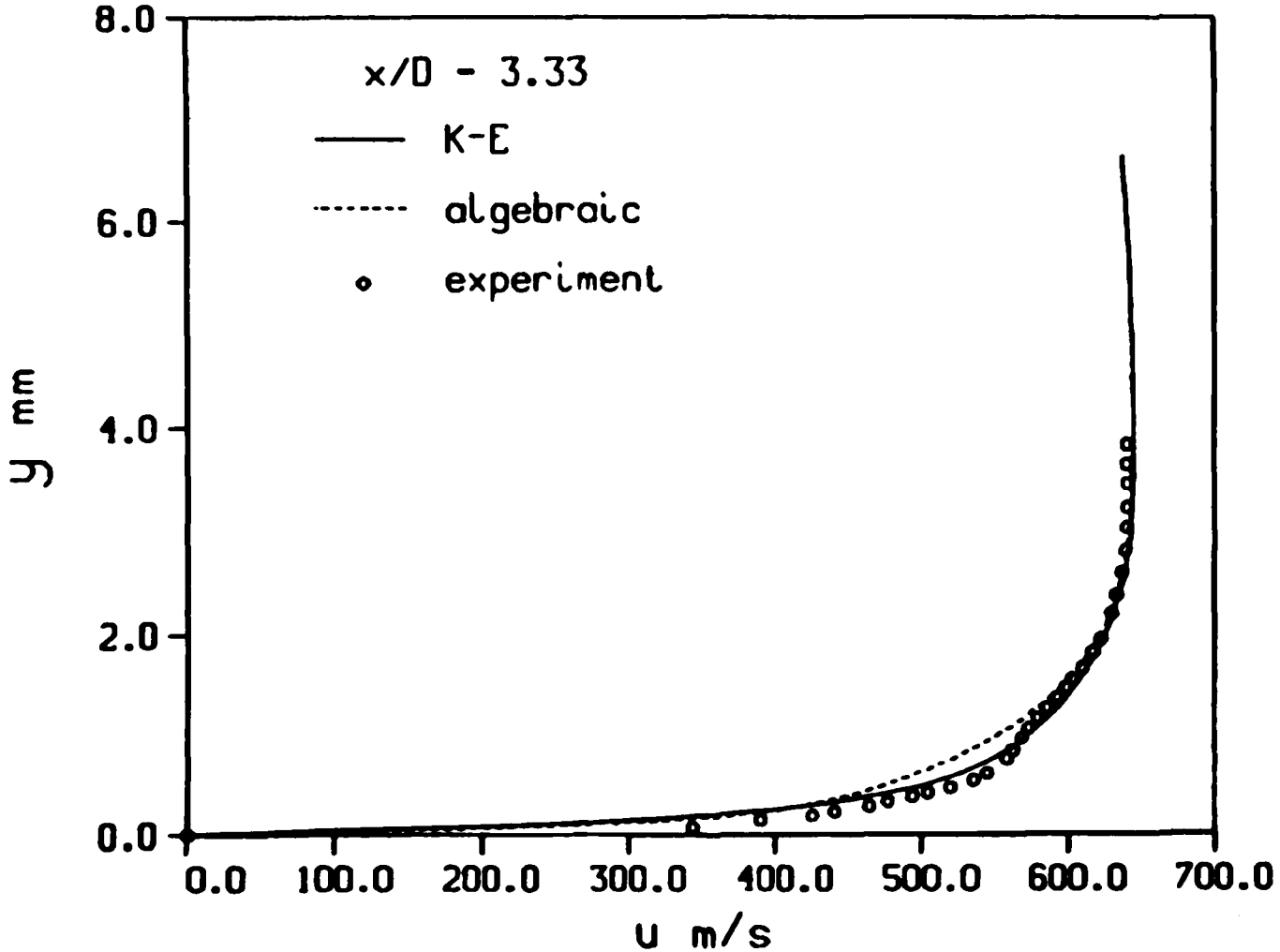

Figure 13. Comparison of PNS Velocity Profile Prediction with Experimental Data

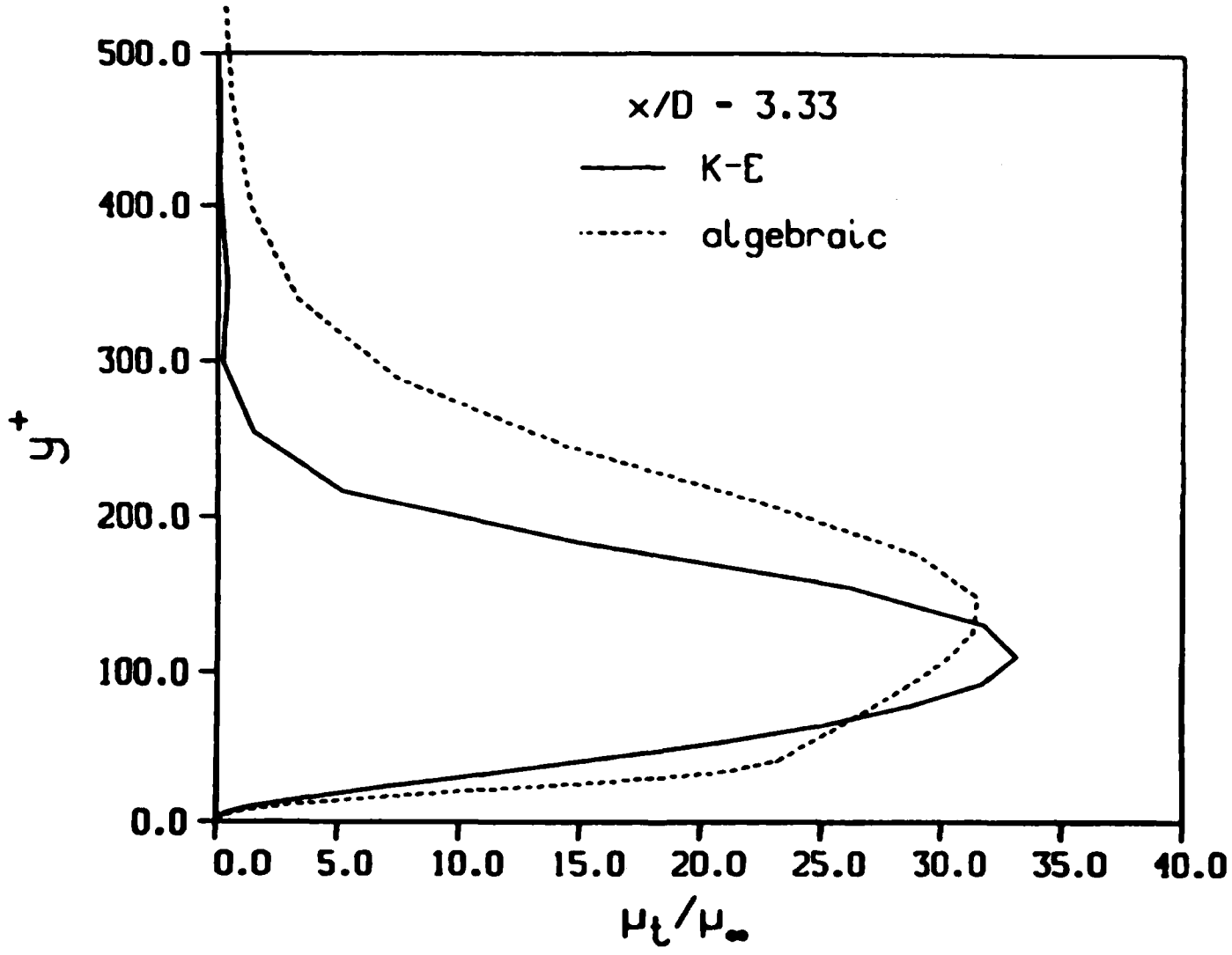

Figure 14. Comparison of K-E and Algebraic Eddy Viscosity Prediction

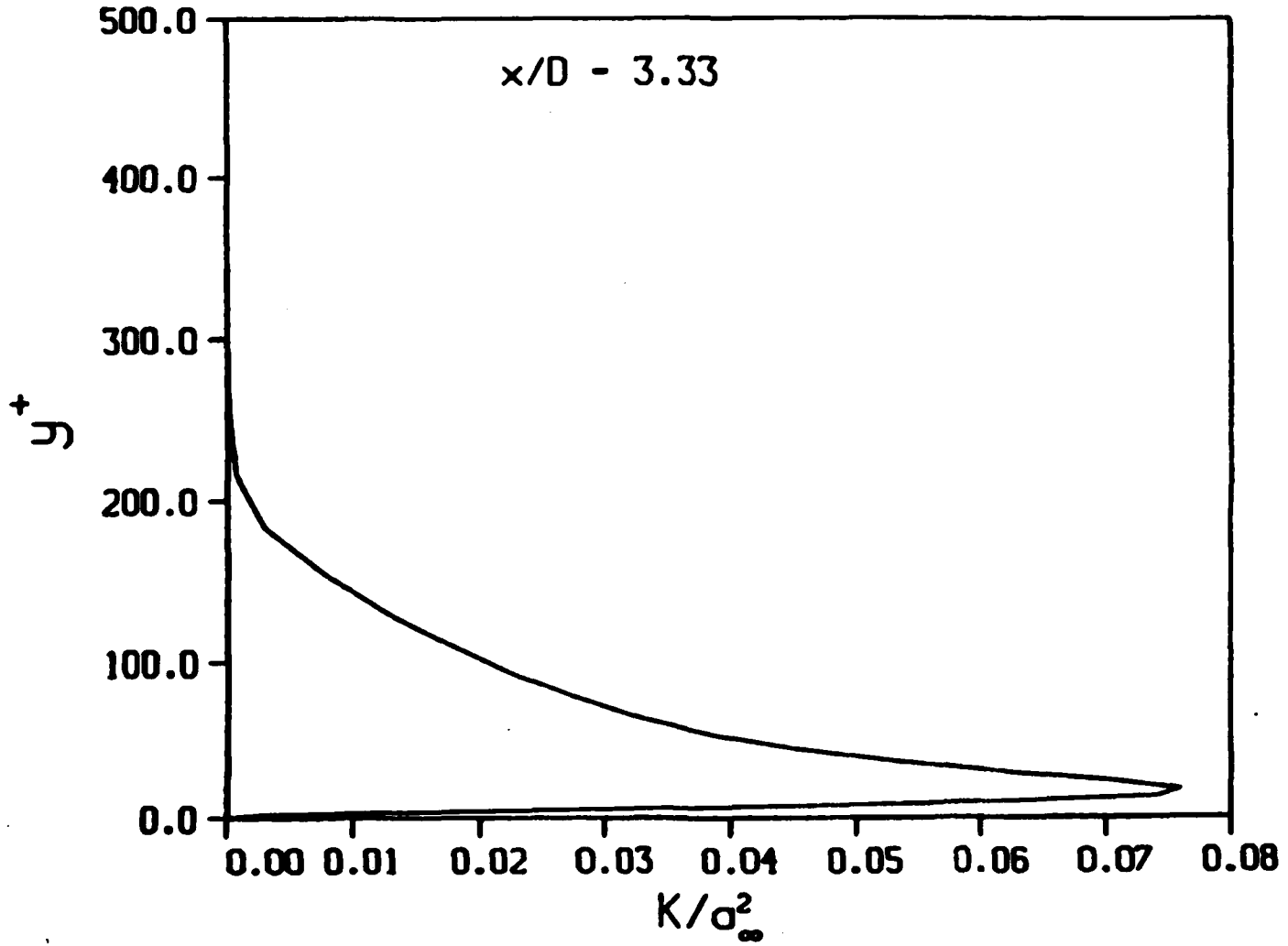

Figure 15. K versus y^+ from PNS Code

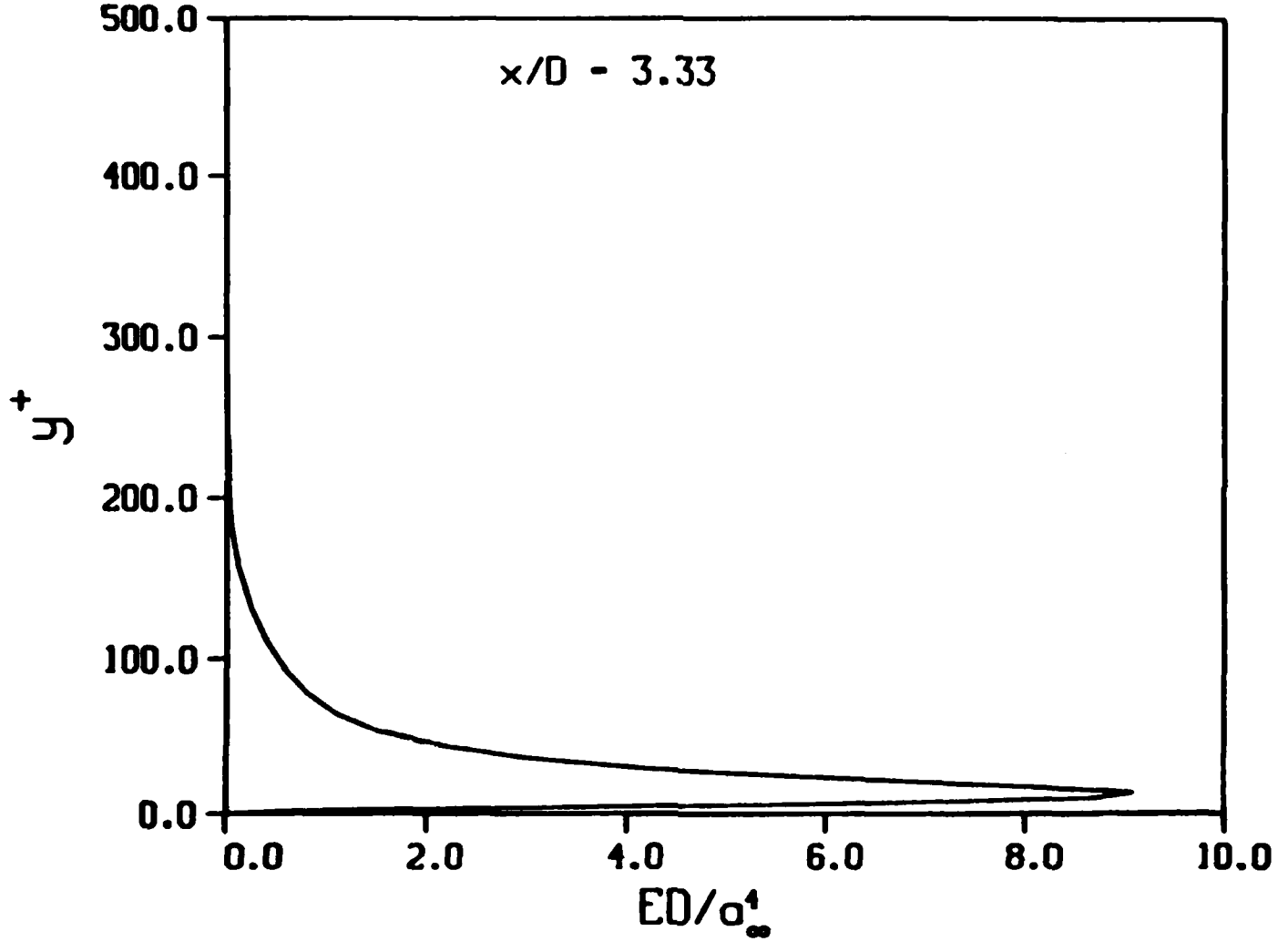

Figure 16. E versus y^+ from PNS Code

REFERENCES

1. Dwyer, H.A., and Sanders, B.R., "Magnus Forces on Spinning Supersonic Cones. Part 1: the Boundary Layer," ARBRL-CR-248, July 1975.

2. Schiff, L.B., and Steger, J.L., "Numerical Simulation of Steady Supersonic Viscous Flow," AIAA Paper 79-0130, January 1979.

3. Beam, R.M., and Warming, R.F., "An Implicit Factored Scheme for Hyperbolic Systems in Conservation-Law Form," Journal of Computational Physics, Vol. 22, 1976.

4. Pulliam, T.H., and Steger, J.L., "On Implicit Finite-Difference Simulations of Three Dimensional Flow," AIAA Journal, Vol. 18, 2, pp. 159-167, February 1980.

5. Nietubicz, C.J., Pulliam, T.H., and Steger, J.L., "Numerical Solution of the Azimuthal-Invariant Thin-Layer Navier-Stokes Equations," AIAA Paper 79-0010, January 1979.

6. Schlichting, H., "Boundary Layer Theory," 7th Edition, McGraw-Hill Book Company, 1979.

7. Launder, B.E., and Spalding, D.B., "Mathematical Modles of Turbulence," Academic Press, Inc., 1972.

8. Rubesin, M.W., "Numerical Turbulence Modeling," AGARD Lecture Series No. 86 on Computational Fluid Dyanmics, April 1977, pp. 3-1 to 3-37.

9. Reynolds, W.C., "Computation of Turbulent Flows," Ann. Rev. Fluic Mech., Vol. 8, pp. 183-208, 1976.

10. Jones, W.P., and Launders, B.E., "The Caluclation of Low Reynolds Number Phenomena with a Two Equation Model of Turbulence," Int. J. Heat and Mass Transfer, Vol. 16, 1973.

11. Van Gulick, P., "Application of the K-E Turbulence Model to a Boundary Layer Solution for Flow About a Spinning Yawed Projectile at Mach 3," Maters Thesis, Mechanical and Aerospace Engineering Department, University of Delaware, June 1983.

12. Van Gulick, P., and Danberg, J.E., "Application of the K-E Turbulence Model to a Boundary Layer Solution for Flow About a Spinning Yawed Projectile at Mach 3," Proceedings, 12th Southeastern Conference on Theoretical and Applied Mechanics, May 1984.

13. Kim, J., "Computations of Three-Dimensional Turbulent Flow with Parabolized Navier-Stokes Equations and K-E Turbulence Model," Masters Thesis, Mechanical and Aerospace Engineering Department, University of Delaware, January 1984.

REFERENCES (Continued)

14. Sahu, J., "Navier-Stokes Computational Study of Axisymmetric Transonic Turbulent Flows with a Two-Equation Model of Turbulence," Ph.D. Dissertation, Mechanical and Aerospace Engineering Department, University of Delaware, June 1984.

15. Cebeci, T., and Smith, A.M.O., "Analysis of Turbulent Boundary Layers," Academic Press, Inc., 1974.

16. Rebesin, M.W., "A One-Equation Model of Turbulence for Use with the Compressible Navier-Stokes Equations," NASA TMX-73, 1976.

17. White, F.M., "Viscous Fluid Flow," McGraw-Hill Book Company, 1974.

18. Schubauer, G.B., and Tchen, C.M., "Turbulent Flow," Turbulent Flow and Heat Transfer, Ed. C.C. Lin, Princeton Series on High Speed Aerodynamics and Jet Propulsion, Princeton University Press, 1959.

19. Chien, K-Y, "Predictions of Channel and Boundary Layer Flows with a Low-Reynolds-Number Turbulence Model," AIAA Journal, Vol. 20, No. 1, 1982.

20. Rotta, J.C., "A Family of Turbulence Models for Three-Dimensional Thin-Shear Layers," Symposium of Turbulent Shear Flows, University Park, Pennsylvania, 1977.

21. Baldwin, B.S., and Lomax, H., "Thin Layer Approximation and Algebraic Model for Separated Turbulent Flows," AIAA Paper 78-257, 1978.

22. Kayser, L.D., and Sturek, W.B., "Experimental Measurements in the Turbulent Boundary Layer of a Yawed, Spinning Ogive-Cylinder Body of Revolution at Mach 3.0. Part II: Data Tabulation," US Army Ballistic Research Laboratory, ARBRL-MR-02813, March 1978.

23. Bradshaw, P., "The Analogy Between Streamline Curvature and Buoyancy in Turbulent Shear Flow," Journal Fluid Mech., Vol. 36, Part I, 1969.

24. Arpaci, V.S., and Larsen, P.S., "Convective Heat Transfer," Prentice-Hall, 1984.

25. Launder, B.E., Priddin, C.H., and Sharma, B.F., "The Calculation of Turbulent Boundary Layers on Spinning and Curved Surfaces," Journal Fluids Engineering, March 1977, pp. 231-239.

26. Steger, J.L., "Implicit Finite-Difference Simulation of Flow About Arbitrary Two-Dimensional Geometries," AIAA Journal, Vol. 16, No. 7, July 1978.

27. Beam, R.M., and Warming, R.F., "An Implicit Factored Scheme for the Compressible Navier-Stokes Equations," AIAA Journal, Vol. 16, No. 4, April 1978.

28. Sturek, W.B., and Schiff, L.B., "Computation of the Magnus Effect for Slender Bodies in Supersonic Flow," AIAA Paper 80-1586CP, August 1980.

29. Schiff, L.B., and Sturek, W.B., "Numerical Simulation of Steady Supersonic Flow Over an Ogive-Cylinder-Boattail Body," AIAA Paper 80-0066, January 1980.

LIST OF SYMBOLS

a = Speed of Sound

c_p = Specific Heat at Constant Pressure

c_μ = Constant in Definition of $\mu_t = c_\mu \bar{\rho}\, \tilde{K}^2/\tilde{E}$

D = Characteristic Body Diameter

d_{ij} = $\dfrac{\partial u_i}{\partial x_j} + \dfrac{\partial u_j}{\partial x_i} - \dfrac{2}{3}\dfrac{\partial u_k}{\partial x_k}\delta_{ij}$ $(i,j,k = 1,2,3)$

E = Modified Turbulent Energy Dissipation Rate (eqn. (40))

e = Total Energy $= e_i + u_i u_i/2$

e_{int} = Internal Energy $= RT/(\gamma-1)$

F = Non-Isotropy Parameter (eqn. (48))

g = Acceleration of Gravity

H = Total Enthalpy $= h + u_i u_i/2$

h = Static Enthalpy $= c_p T$

J = Jacobian of Coordinate Transformation

K = Turbulent Kinetic Energy

K_p = Constant (eqn. (46))

k = Thermal Conductivity

L = A Turbulent Length Scale

ℓ = Prandtl Mixing Length

M = Mach Number

P = Production Term in K Equation

Pr = Molecular Prandtl Number

p = Pressure

$\vec{q}$ = Vector of Dependent Variables

q_j = Heat Flux

R = Gas Constant

Re	=	Reynolds Number
Ri	=	Richardson Number
r	=	Radius of Axisymmetric Body
T	=	Temperature
t	=	Time
U,V,W	=	Contravariant Velocities
u_i	=	Velocity Component (i = 1,2,3)
u_τ	=	Wall Shear Velocity = $(\tau_w/\rho)^{1/2}$
u,v,w	=	Velocity Components
V_Θ	=	Velocity on a Curved Streamline (eqn. (67))
x_i	=	Coordinates (i = 1,2,3)
x,y,z	=	Coordinates
y^+	=	Non-Dimensional Wall Coordinate $u_\tau y/\nu$

Greek Symbols

α	=	Angle of Attack
γ	=	Ratio of Specific Heats
δ	=	Boundary Layer Thickness
δ_{ij}	=	Kronnecker Delta
ε	=	Physical Turbulent Energy Dissipation Rate
κ	=	von Karman Constant ≈ 0.4
λ	=	Wake Constant ≈ 0.09
μ	=	Molecular Coefficient of Viscosity
μ_t	=	Turbulent Eddy Viscosity
ν	=	Kinematic Viscosity = μ/ρ
ξ,η,ζ	=	Transformed Coordinate Variables
ρ	=	Density

σ_ε = Effective Prandtl Number in the Dissipation Equation

σ_k = Effective Prandtl Number in the Kinetic Energy Equation

τ_{ij} = Molecular Stress Tensor

ϕ = Circumferential Angle

$*$ = Constant (See equns. (44) and (45))

Ω = Spin Rate

ω = Vorticity

Superscripts

$\sim$ = Mass-Weighted Time Average

$-$ = Time Average

$'$ = Fluctuating Part in Mass-Weighted Time Average ($a_i = a_i + \tilde{a}_i'$)

$''$ = Fluctuating Part in Time Average ($a_i = \bar{a} + a''$)

$+$ = Non-Dimensional Wall Variable

$\rightarrow$ = Vector

Subscripts

t = Turbulent

∞ = Freestream

w = Wall

DISTRIBUTION LIST

No. of Copies	Organization
12	Administrator Defense Technical Info Center ATTN: DTIC-DDA Cameron Station Alexandria, VA 22304-6145
1	HQDA DAMA-ART-M Washington, DC 20310
1	Commander US Army Materiel Command ATTN: AMCDRA-ST 5001 Eisenhower Avenue Alexandria, VA 22333-0001
8	Commander Armament R&D Center US Army AMCCOM ATTN: SMCAR-TDC SMCAR-TSS SMCAR-LCA-F Mr. D. Mertz Mr. E. Falkowski Mr. A. Loeb Mr. R. Kline Mr. S. Kahn Mr. H. Hudgins Dover, NJ 07801
1	Commander US Army Armament, Munitions and Chemical Command ATTN: AMSMC-LEP-L Rock Island, IL 61299
1	Director Benet Weapons Laboratory Armament R&D Center US Army AMCCOM ATTN: SMCAR-LCB-TL Watervliet, NY 12189
1	Commander US Army Armament, Munitions and Chemical Command ATTN: SMCAR-ESP-L Rock Island, IL 61299

No. of Copies	Organization
1	Commander US Army Aviation Research and Development Command ATTN: AMSAV-E 4300 Goodfellow Blvd St. Louis, MO 63120
1	Director US Army Air Mobility Research and Development Command Ames Research Center Moffett Field, CA 94035
1	Commander US Army Communications - Electronics Command ATTN: AMSEL-EB Fort Monmouth, NJ 07703
1	Commander ERADCOM Technical Library ATTN: DELSD-L (Reports Section) Fort Monmouth, NJ 07703-5301
3	Commander US Army Missile Command Research, Development & Engineering Center ATTN: AMSMI-RD Dr. Bill Walker Mr. R. Deep Redstone Arsenal, AL 35898
1	Director US Army Missile & Space Intelligence Center ATTN: AIAMS-YDL Redstone Arsenal, AL 35898-5000
1	Commander US Army Tank Automotive Command ATTN: AMSTA-TSL Warren, MI 48397-5000
1	Director US Army TRADOC Systems Analysis Activity ATTN: ATAA-SL White Sands Missile Range, NM 88002

DISTRIBUTION LIST

No. of Copies	Organization
1	Commander US Army Research Office P. O. Box 12211 Research Triangle Park, NC 27709
1	Commander US Naval Air Systems Command ATTN: AIR-604 Washington, DC 20360
2	Commander David W. Taylor Naval Ship Research and Development Center ATTN: Dr. S. de los Santos Mr. Stanley Gottlieb Bethesda, Maryland 20084
2	Commander US Naval Surface Weapons Center ATTN: Dr. T. Clare, Code DK20 Dr. F. Moore Dahlgren, VA 22448-5000
1	Commander US Naval Surface Weapons Center ATTN: Dr. U. Jettmar Silver Spring, MD 20902-5000
1	Commander US Naval Weapons Center ATTN: Code 3431, Tech Lib China Lake, CA 93555
1	Commander US Army Development and Employment Agency ATTN: MODE-TED-SAB Fort Lewis, WA 98433
1	Director NASA Langley Research Center ATTN: NS-185, Tech Lib Langley Station Hampton, VA 23365
2	Commandant US Army Infantry School ATTN: ATSH-CD-CSO-OR Fort Benning, GA 31905
1	AFWL/SUL Kirtland AFB, NM 87117
1	Air Force Armament Laboratory ATTN: AFATL/DLODL Eglin AFB, FL 32542-5000
3	Sandia Laboratories ATTN: Technical Staff, Dr. W.L. Oberkampf Aeroballistics Division 5631, H.R. Vaughn Dr. F. Blottner Albuquerque, NM 87184
3	Director NASA Ames Research Center ATTN: MS-227-8, L. Schiff MS-202A-14, D. Chaussee M. Rai Moffett Field, CA 94035
1	Massachusetts Institute of Technology ATTN: Tech Library 77 Massachusetts Avenue Cambridge, MA 02139
1	Virginia Polytechnic Institute & State University ATTN: Dr. Clark H. Lewis Department of Aerospace & Ocean Engineering Blacksburg, VA 24061
1	University of Delaware Mechanical and Aerospace Engineering Department ATTN: Dr. J. E. Danberg Newark, DE 19711

DISTRIBUTION LIST

10 Central Intelligence Agency
Office of Central Reference
Dissemination Branch
Room GE-47 HQS
Washington, DC 20502

Aberdeen Proving Ground

Dir, USAMSAA
ATTN: AMXSY-D
AMXSY-MP, H. Cohen

Cdr, USATECOM
ATTN: AMSTE-TO-F

Cdr, CRDC, AMCCOM,
ATTN: SMCCR-RSP-A
SMCCR-MU
SMCCR-SPS-IL

USER EVALUATION SHEET/CHANGE OF ADDRESS

This Laboratory undertakes a continuing effort to improve the quality of the reports it publishes. Your comments/answers to the items/questions below will aid us in our efforts.

1. BRL Report Number_____ Date of Report_____

2. Date Report Received_____

3. Does this report satisfy a need? (Comment on purpose, related project, or other area of interest for which the report will be used.)_____

4. How specifically, is the report being used? (Information source, design data, procedure, source of ideas, etc.)_____

5. Has the information in this report led to any quantitative savings as far as man-hours or dollars saved, operating costs avoided or efficiencies achieved, etc? If so, please elaborate._____

6. General Comments. What do you think should be changed to improve future reports? (Indicate changes to organization, technical content, format, etc.)

CURRENT ADDRESS

Name

Organization

Address

City, State, Zip

7. If indicating a Change of Address or Address Correction, please provide the New or Correct Address in Block 6 above and the Old or Incorrect address below.

OLD ADDRESS

Name

Organization

Address

City, State, Zip

(Remove this sheet along the perforation, fold as indicated, staple or tape closed, and mail.)

FOLD HERE

Director
U.S. Army Ballistic Research Laboratory
ATTN: SLCBR-DD-T
Aberdeen Proving Ground, MD 21005-5066

NO POSTAGE
NECESSARY
IF MAILED
IN THE
UNITED STATES

OFFICIAL BUSINESS
PENALTY FOR PRIVATE USE, $300

BUSINESS REPLY MAIL
FIRST CLASS PERMIT NO 12062 WASHINGTON, DC
POSTAGE WILL BE PAID BY DEPARTMENT OF THE ARMY

Director
U.S. Army Ballistic Research Laboratory
ATTN: SLCBR-DD-T
Aberdeen Proving Ground, MD 21005-9989

FOLD HERE

END

DTIC

8-86